



Cite as
Nano-Micro Lett.
(2025) 17:3

Received: 20 June 2024
Accepted: 27 July 2024
© The Author(s) 2024

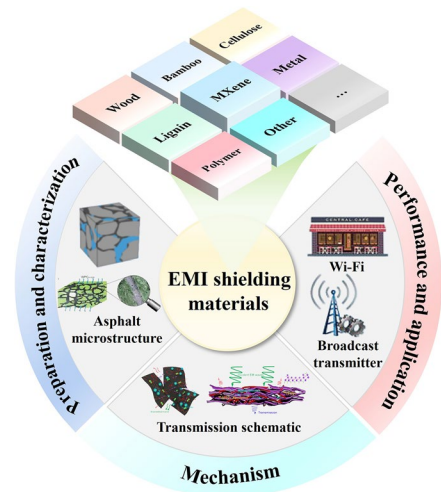
Advanced Functional Electromagnetic Shielding Materials: A Review Based on Micro-Nano Structure Interface Control of Biomass Cell Walls

Yang Shi¹, Mingjun Wu¹, Shengbo Ge¹, Jianzhang Li² ✉, Anoud Saud Alshammari³, Jing Luo¹ ✉, Mohammed A. Amin⁴, Hua Qiu⁵, Jinxuan Jiang¹, Yazeed M. Asiri⁴, Runzhou Huang¹, Hua Hou^{6,7}, Zeinhom M. El-Bahy⁸, Zhanhu Guo⁶ ✉, Chong Jia¹, Kaimeng Xu⁹ ✉, Xiangmeng Chen¹⁰ ✉

HIGHLIGHTS

- The advantages of biomass materials for electromagnetic interference (EMI) shielding are analyzed, the mechanism of EMI shielding is summarized, and the factors affecting EMI shielding are analyzed systematically.
- Various biomass materials (wood, bamboo, lignin, cellulose) were modified to obtain unique structures and improve EMI shielding performance.
- The problems encountered in the application of biomass materials for EMI shielding are summarized, and the potential development and application in the future are prospected.

ABSTRACT Research efforts on electromagnetic interference (EMI) shielding materials have begun to converge on green and sustainable biomass materials. These materials offer numerous advantages such as being lightweight, porous, and hierarchical. Due to their porous nature, interfacial compatibility, and electrical conductivity, biomass materials hold significant potential as EMI shielding materials. Despite concerted efforts on the EMI shielding of biomass materials have been reported, this research area is still relatively new compared to traditional EMI shielding materials. In particular, a more comprehensive study and summary of the factors influencing biomass EMI shielding materials including the pore structure adjustment, preparation process, and micro-control would be valuable. The preparation methods and characteristics of wood, bamboo, cellulose and lignin in EMI shielding field are critically discussed in this paper, and similar biomass EMI materials are summarized and analyzed. The composite methods and fillers of various biomass materials were reviewed. this paper also highlights the mechanism of EMI shielding as well as existing prospects and challenges for development trends in this field.



KEYWORDS Biomass materials; Electromagnetic interference shielding; Micro-nano structure interface control; Conductivity

Yang Shi and Mingjun Wu have been contributed equally to this work and act as co-first authors.

✉ Jianzhang Li, lijzh@bjfu.edu.cn; Jing Luo, jingluo@njfu.edu.cn; Zhanhu Guo, zhanhu.guo@northumbria.ac.uk; Kaimeng Xu, xukm007@163.com; Xiangmeng Chen, xmchen0610@163.com

¹ Co-Innovation Center of Efficient Processing and Utilization of Forest Resources, College of Materials Science and Engineering, Nanjing Forestry University, Nanjing 210037, People's Republic of China

² State Key Laboratory of Efficient Production of Forest Resourced, Beijing Forestry University, Qinghua East Road 35, Haidian District, Beijing 100083, People's Republic of China

³ Department of Physics, Faculty of Sciences-Arar, Northern Border University, Arar 91431, Saudi Arabia

⁴ Department of Chemistry, College of Science, Taif University, P.O. Box 11099, 21944 Taif, Saudi Arabia



1 Introduction

The universal practice of mobile phones [1–3], computers [4], and other electronic devices [5–11] has transformed human society with unprecedented convenience [12–15]. However, this convenience comes at a cost, as these electronic devices are also responsible for electromagnetic interference (EMI) and pollution [16–20]. In fact, The World Health Organization (WHO) has listed electromagnetic radiation as the fourth largest source of environmental pollution after water pollution, air pollution and noise pollution. This escalating issue has sparked significant public concern [21]. It was found that electromagnetic pollution can obstruct the normal functioning of electronic equipment which would lead to malfunctions and potential data leakage. Additionally, it poses significant health risks to individuals such as headaches, insomnia, and lethargy [22, 23]. Therefore, it is crucial to prioritize the evolution of materials with efficient electromagnetic shielding to alleviate these risks while maintaining their properties for respective applications [24–27]. Figure 1a–c shows the potential source of electromagnetic waves in daily life and relevant studies published in the past few years. In recent years, the research on EMI shielding materials has gradually increased, but there are still relatively few studies on biomass EMI shielding materials. With people's attention to electromagnetic pollution and environment, biomass EMI materials have been studied relatively more in the past two years. This allows us to see the prospect of biomass EMI shielding materials, this paper will introduce the current biomass EMI shielding materials preparation, characteristics for the reference of researchers.

In the past, studies of electromagnetic shielding materials focused on metal oxides [28–30], metals [25, 31], carbon-based materials [32–35], metal carbide [36], sulfide [37], magnetic materials, and polymer shielding materials (Fig. 2) [38–43]. Among these, metals (e.g., Fe, Ag, Ni, Cu, and Al) and their compounds have been extensively studied for their effectiveness in shielding electromagnetic

and electrostatic fields [44–46]. It was found that transition metal sulfides exhibit strong electrochemical activity, higher specific capacitance, and enhanced conductivity [47, 48]. However, challenges related to the strong electromagnetic waves (EMWs) that has caused secondary interference, depletion of metal resources, high density, susceptibility to corrosion, and processing difficulties have constrained their widespread application [37, 49–51]. Magnetic materials exhibit strong absorption and attenuation properties when exposed to low-frequency electromagnetic radiation [52, 53]. However, their effectiveness diminishes when exposed to high-frequency electromagnetic radiation, and their thickness further restricts their practical application in electromagnetic shielding [54].

Recently, the primary research direction for polymer shielding materials centers around polythiophene (PT), polyurethane (PU), polypyrrole (PPy), polyacetylene (PA), and other polymers with conjugated π -bonds [55–57]. These materials have secured substantial spotlight due to their outstanding performance, which includes high efficiency, lightweight, corrosion resistance, and excellent processing capabilities [58]. For example, Sun et al. used electrostatic assembly and molding to load Ti_3C_2 onto the surface of polystyrene particles. Due to the high conductivity of MXene and its efficient conductive network in the polystyrene matrix, the polystyrene/ Ti_3C_2 composite was constructed with a high conductivity of 1081 S m^{-1} and an electromagnetic interference shielding effectiveness (EMI SE) of 64 dB [59]. However, the preparation process is complex, and the individual materials do not possess exceptional electromagnetic shielding performance. As such, large amount of conductive fillers is usually added, which in turn limits its application in electromagnetic shielding and compromises the mechanical properties of the material [60–62].

On the other hand, carbon-based materials like reduced graphene oxide (RGO), carbon nanofibers (CNF), carbon nanotubes (CNT), and their composite materials [63–68] exhibit excellent electrical conductivity, high dielectric

⁵ Shaanxi Key Laboratory of Macromolecular Science and Technology, School of Chemistry and Chemical Engineering, Northwestern Polytechnical University, Xi'an, Shaanxi 710072, People's Republic of China

⁶ Integrated Composites Lab, Department of Mechanical and Construction Engineering, Northumbria University, Newcastle Upon Tyne NE1 8ST, UK

⁷ College of Materials Science and Engineering, Taiyuan University of Science and Technology, Taiyuan 030024, People's Republic of China

⁸ Department of Chemistry, Faculty of Science, Al-Azhar University, Nasr City, Cairo 11884, Egypt

⁹ Yunnan Provincial Key Laboratory of Wood Adhesives and Glued Products, International Joint Research Center for Biomass Materials, Southwest Forestry University, Kunming 650224, People's Republic of China

¹⁰ School of Science, Henan Agricultural University, Zhengzhou 450002, People's Republic of China

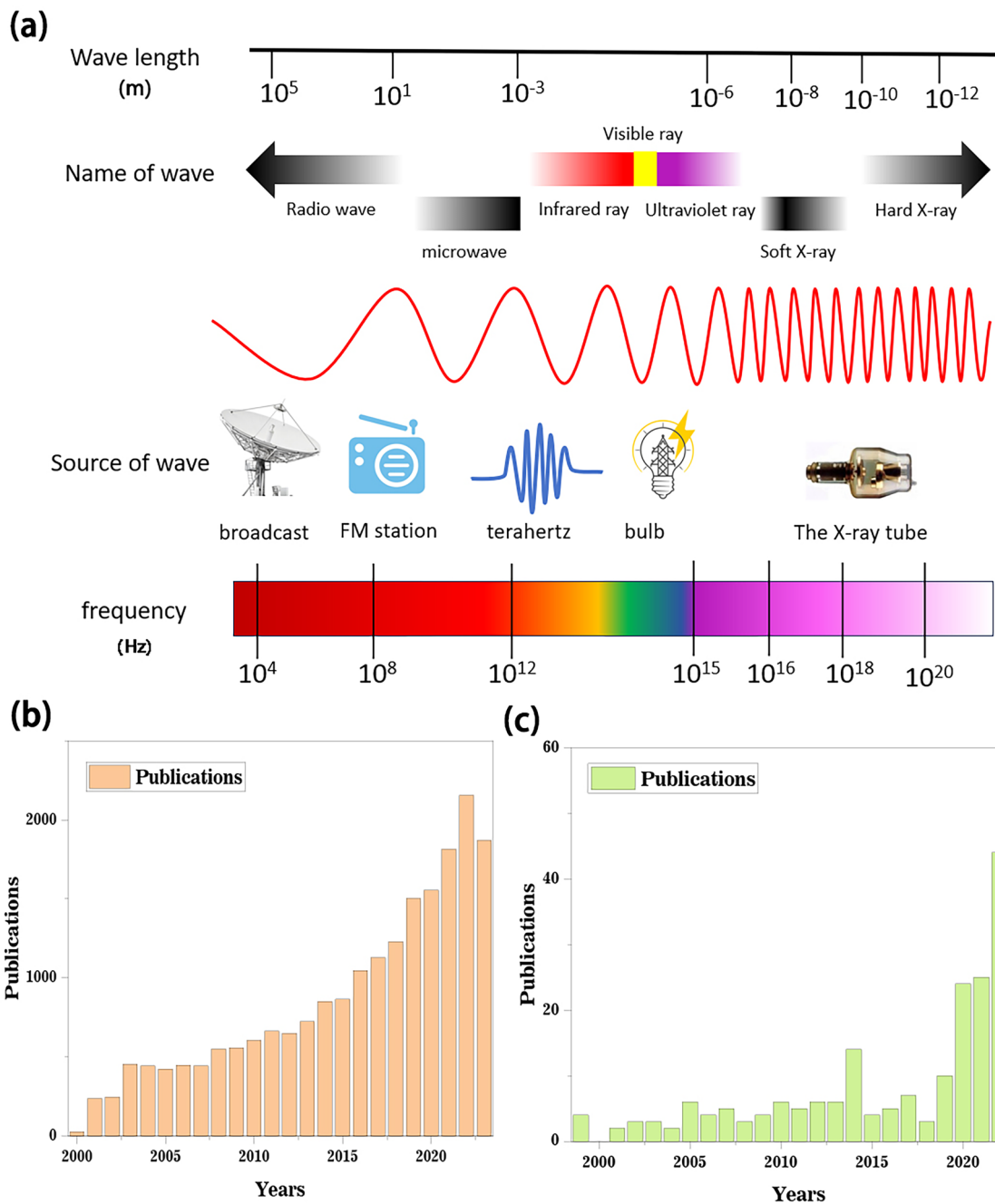


Fig. 1 **a** Objects that often cause electromagnetic waves in life. **b** Articles published on electromagnetic shielding in the past few years. **c** Articles published on electromagnetic shielding of biomass in the two decades

loss, specific surface area, outstanding chemical stability, and large aspect ratio, suggesting their potential use in electromagnetic shielding applications [69–72]. For example, Li et al. successfully constructed a CNT/SiC coaxial three-dimensional porous composite sponge using a low-temperature growth strategy. Its comprehensive performance

is excellent, low density, super elasticity, excellent thermal resistivity, EMI of 75.7 dB in the X-band [73]. However, their relatively high production costs, expensive manufacturing equipment, and complex processing methods present challenges in meeting large-scale production requirements [60, 74].

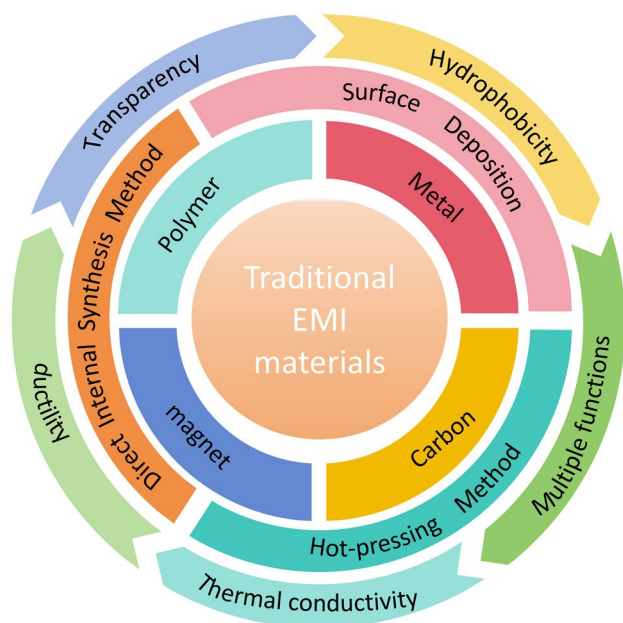


Fig. 2 Traditional EMI shielding materials, preparation methods and properties

1.1 Application of Biomass Materials in Electromagnetic Shielding Field

The call for effective electromagnetic shielding materials has elevated in recent years owing to resource scarcity and growing environmental concerns. Unfortunately, existing traditional materials have struggled to meet practical demand, but problems such as their difficulty in processing, non-degradability, and depletion of raw materials have led to the exploration of alternative options [75–77]. Biomass materials have garnered attention due to their low cost, sustainability, lightweight nature, and porous hierarchical structure, making them a promising alternative to traditional EMI shielding materials [78–81]. Biomass-based multi-function electromagnetic shielding materials not only effectively shield electromagnetic waves, but also have other functions, such as electrical conductivity, significant flame retardancy and antibacterial activity. Compared with traditional materials, biomass materials can adjust their structure through different treatment and processing methods, for example, by optimizing the pore structure, shape, size and distribution to improve the material's absorption loss and multiple reflection attenuation, thereby enhancing its shielding effect. Some common biomass materials used for electromagnetic shielding are wood, bamboo, lignin, and cellulose (Fig. 3).

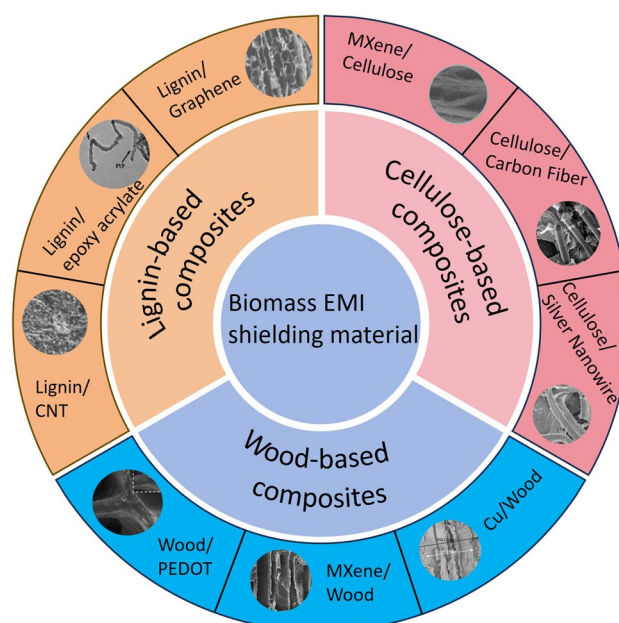


Fig. 3 Various types of biomass materials for EMI shielding field, with wood, cellulose, lignin as an example

In particular, wood-based composites are known for their excellent electrical conductivity, lightweight and stable structure, and porous nature, making them a strong candidate for EMI shielding.

Wood-based materials such as wood metal composites, wood polymer composites, and wood-derived carbon composites are employed in EMI shielding [82–84]. Additionally, graphene is a demanding option for EMI materials due to its extensive surface area, exceptional electrical conductivity, mechanical flexibility, and other remarkable physical and chemical properties [85]. For instance, Guo et al. prepared Wood/Cu-Fe₃O₄@graphene/Ni composites. The conductivity of the composite was improved by adding Fe₃O₄@graphene with high crystallinity and purity. The micro and nano particles are evenly distributed on the surface of the wood, forming a dense coating. The EMI SE of the composite material is 96.79 dB [86]. Furthermore, nanocellulose (i.e., a natural polymer derived from cellulose), which has a high specific surface area and impressive mechanical properties [87, 88], shows promise for application in biomass EMI shielding materials [31, 89, 90]. For example, Han et al. utilized magnetic Ni particles to modify graphene oxide and nano-fibrillated cellulose in order to create EMI shielding films. Their research

found that EMI shielding effectiveness (SE) could reach 32.2 dB [91]. Additionally, Zhang et al. utilized bamboo as a renewable biomass material to prepare a bamboo-plastic composite electromagnetic shielding material. By filling high-density polyethylene (HDPE) with nickel-plated bamboo, they achieved an impressive EMI SE of 82 dB [92]. Moreover, cellulose and lignin were highlighted for their wide availability, low cost, and porous nature [93]. Exploration of a wide range of materials including wood-based composites, graphene-enhanced polymers, and bamboo-plastic composites [94], demonstrates the potential for high levels of EMI shielding effectiveness. These innovative approaches address the urgent need for effective EMI shielding and demonstrate the potential of using renewable biomass materials to develop sustainable solutions for mitigating electromagnetic pollution.

Currently, there is a growing concern for the environment and an increased awareness of the importance of developing effective wearable protective materials and EMI shielding materials [95, 96]. For example, Yuan et al. have documented the development of a highly elastic, stretchy polyurethane nanofiber fabric coated with $Ti_3C_2T_x$, which maintains an EMI SE of over 20 dB and exhibits stable mechanical properties [97]. Cao et al. have also introduced a composite film utilizing CNTs/MXene/CNFs to create wearable yet flexible EMI shielding materials through a sandwiching process [98]. Similarly, Zhao et al. obtained the polyacrylamide/2-hydroxypropyl trimethylammonium chloride chitosan (PAM/HACC) interpermeable network by heat-initiated polymerization through the strong electrostatic interaction and hydrogen bonding between the positively charged group on HACC and the PAM polymer chain. It was used as skeleton in situ polymerization of PPy. It has flexibility, good mechanical strength, and EMI SE up to 40 dB [99]. Biomass materials have delineated a remarkable possibility for EMI shielding due to their rich interface and porous structure. This allows them to achieve EMI SE of over 20 dB. Furthermore, these materials can be tailored to provide resistance to mildew, electrical conductivity, and flame retardancy, making them applicable for use in various extreme environments [68, 100]. Despite their promising characteristics, biomass-based EMI shielding materials have limited reported applications, hence suggesting significant untapped potential [101–103]. Therefore, there is an urgent need to explore and review existing works related to these promising biomass materials for EMI shielding.

This paper comprehensively reviews preparation methods, material structure design, EMI shielding mechanisms, and other relevant aspects of various biomass materials. A detailed summary of recent research on different types of biomass EMI shielding materials was proposed, along with an analysis of the associated challenges, issues, and future trends. The review emphasizes recent advancements and noteworthy accomplishments in applying biomass-based materials in electromagnetic shielding. It is anticipated that this review will significantly influence the development of environmentally friendly, lightweight, and sustainable electromagnetic shielding materials. The content provided would inspire contemporary design for the creation of relevant biomass electromagnetic shielding materials and propose new possibilities for the design of green yet degradable biomass materials with excellent electromagnetic shielding properties that can be used in various industries such as construction, medical treatment, and clothing [104–106].

2 Mechanism of Electromagnetic Shielding

When a magnetic field changes, it causes an electric field to change. These fields oscillate vertically in the same direction and create electromagnetic waves (EMW) in the changing field [107, 108]. Unlike other types of wave propagation, EMWs transfer energy efficiently without a medium. The resulting electromagnetic radiation from EMWs has an irreversible impact on the surrounding environment. This effect is known as EMI. EMI shielding involves using specific materials to isolate EMWs and effectively control their transmission in a certain area. The shielding mechanism includes internal multiple reflections, reflection, and absorption (Fig. 4).

2.1 Shielding Effectiveness

EMI SE represents the primary indicator to evaluate the electromagnetic shielding effect of materials. The EMI SE principally relies on the internal multiple reflection loss, absorption loss and reflection loss of electromagnetic shielding material.

EMI SE defines the ratio of the intensity of the incident electromagnetic field to the emitted electromagnetic field and is expressed by Eq. (1) [109–111]:

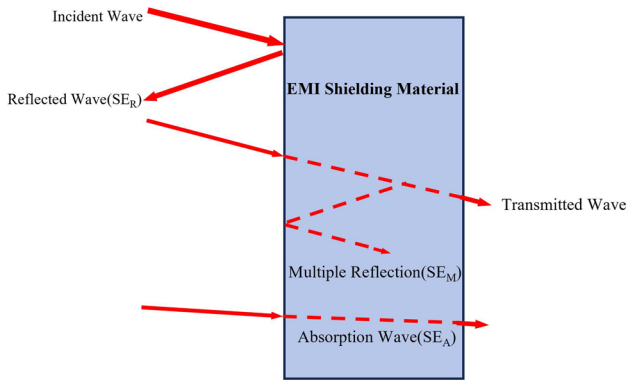


Fig. 4 Electromagnetic shielding mechanism diagram of EMI shielding material

$$SE = 10 \log \left(\frac{P_i}{P_t} \right) = 20 \log \left(\frac{H_i}{H_t} \right) = 20 \log \left(\frac{E_i}{E_t} \right) \quad (1)$$

where P_t denotes the transmitted EMW power, P_i is the incident EMW power, H_i represents the incident EMW magnetic field, H_t refers to the transmitted EMW magnetic field, E_t denotes the transmitted EMW electric field and E_i is the incident EMW electric field.

According to Serkunov’s theory, the EMI SE can be defined in Eq. (2) [112]:

$$SE_T = SE_R + SE_A + SE_M \quad (2)$$

where SE_T is the total EMI shielding effectiveness, SE_R denotes the surface reflection, SE_A represents the internal absorption and SE_M refers to the multiple internal reflection.

Surface reflection (SE_R) is influenced by a mismatch among the intrinsic impedance of the EMI shielding material and the free-space impedance. SE_R can be calculated by Eq. (3) [113–115]:

$$SE_R = 168.2 + 10 \log \left(\frac{\sigma_{rel}}{f \mu_{rel}} \right) \quad (3)$$

where f is the frequency of the incident battery wave, σ_{rel} denotes the relative conductivity, and μ_{rel} refers to the relative permeability.

Multiple internal reflection (SE_M) is caused by macroscopic multiple reflections within the two shielding layer interfaces. SE_M can be obtained via Eq. (4) as follows [116–119]:

$$SE_M = 20 \log \left(1 - 10^{-\frac{SE_A}{10}} \right) \quad (4)$$

When $SE_T > 15$ dB, SE_M can be ignored [120].

Internal absorption (SE_A) represents the attenuation of electromagnetic energy influenced by magnetic loss and dielectric loss in the EMI shield. The calculation is demonstrated in Eq. (5) as follows [121, 122]:

$$SE_A = 131.43t \sqrt{f \sigma_{rel} \mu_{rel}} \quad (5)$$

where t denotes the thickness of the EMI shield.

2.2 Effect of Porous Structure of Biomass Materials on EMI Shielding Properties

Figure 5 demonstrates the electromagnetic shielding mechanism of biomass materials. When an electromagnetic wave comes to the shielding material surface, a portion of the wave is reflected due to the mismatch between the impedance of the travelling medium its inherent impedance, hence reducing the energy that passes through the interface. The remaining energy is absorbed by the shielding material and converted into heat, this further reducing the EMW. The remaining electromagnetic wave is gradually attenuated

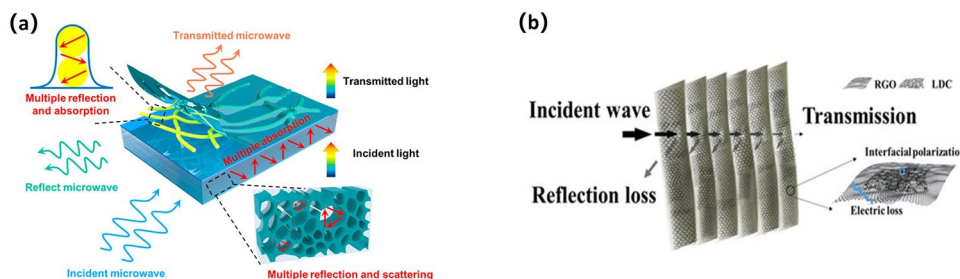


Fig. 5 **a** Diagram of electromagnetic shielding mechanism of AgNW@MXene/Wood [125]. **b** Microwave attenuation mechanisms of Graphene/lignin-derived carbon [126]

through multiple reflections inside the shield, with only a small amount passing through the material [107, 123, 124]. The higher the conductivity and magnetic permeability of the shielding material, the better the shielding effect. In addition, high-frequency electromagnetic waves have a skin effect in conductive media, resulting in energy loss and reduced field amplitude, making it easier to shield. Overall, the microstructure of biomass materials can effectively shield EMI through the reconfiguration and scattering of EMWs. Adding conductive fillers to biomass materials, such as carbon fiber and graphene, will form a conductive mesh structure. Stacking different polymer composite layers can optimize impedance matching, improve absorption losses and multiple reflection attenuation, and thus enhance the shielding effect. Biomass materials such as crop straw can be converted into conductive carbon after high temperature carbonization, which can improve the EMI SE of composite materials. The porous structure of biomass materials combined with various reflection and absorption processes would block the majority of the electromagnetic waves passing through the material.

Figure 6 illustrates the factors that affect reflection, absorption, and multiple reflections in EMI shielding. By adding conductive fillers, stacking different composite layers and carbonization treatment, the biomass material has high magnetic conductivity. The composite material can selectively shield EMW in EMI shielding field. The EMI SE of hybrid polymer composites is influenced by several properties and factors, including the magnetic and electrical properties of fillers, fibers, and polymer substrates, as well as the manufacturing methods and composite structure. Composites typically have a combined shielding

mechanism of reflection and absorption at the interface, followed by absorption. As electromagnetic waves propagate through the material, they scatter at scattering centers, interfaces, or defects, leading to electromagnetic radiation attenuation [127].

The EMWs inside the material decay due to a variety of mechanisms, mainly including dielectric and magnetic losses, which convert electromagnetic energy into heat. Dielectric loss is when EMWs pass through biomass material, the atoms or molecules in the medium are vibrated by the electric field, reducing EMW propagation. Magnetic loss is the energy loss caused by the change in magnetic field energy during EMW propagation, which is converted into heat energy, thereby improving EMW absorption. In experiments, multilayer shielding structures are usually designed to achieve impedance matching. Interfacial polarization is the polarization charge induced at the material interface due to uneven charge distribution, which will produce a dissipative effect under an alternating electric field. Moreover, Polarization loss is the energy loss caused by dielectric polarization under electric field action [128]. In experiments, multilayer shielding structures are usually designed to achieve impedance matching. Improved impedance matching can reduce the EMW reflection on the material surface so that the EMWs enter the material and are absorbed [129]. Through the application of these mechanisms, we can better prepare biomass composites with high significant EMI SE. For example, the overall absorption effect can be enhanced by designing multilayer structures that take advantage of the impedance and absorption characteristics of different materials.

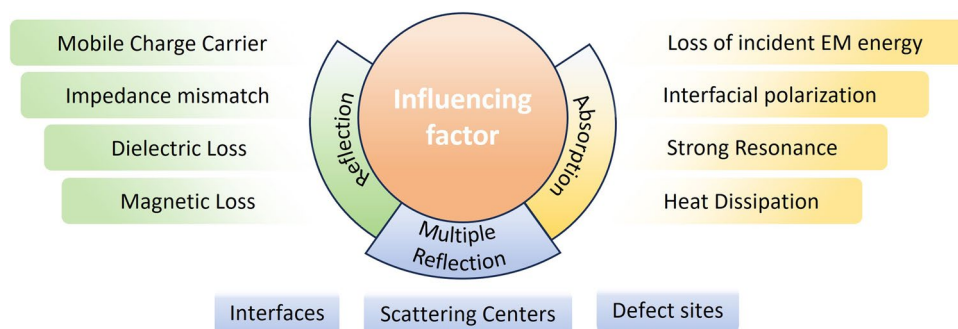


Fig. 6 Factors affecting reflection, absorption and multiple reflection in EMI shielding

3 Preparation and Characterization

There is a significant amount of literature on the EMI shielding properties of biomass materials. A summary of various biomass materials used for electromagnetic shielding is available. The following section will describe the preparation and properties of biomass materials for EMI shielding.

3.1 Wood and Its Derivatives

Wood represents an environmentally friendly yet biodegradable material with a large specific surface area and rich layered porous structure [130, 131]. The presence of these pores improves the impedance matching performance, improves the absorption efficiency of EMWs and facilitates multiple EMWs reflection in the pores. Besides, the wood surface also consists of abundant active hydroxyl groups, which provides an ideal environment for binding of inorganic particles [132–134].

3.1.1 MXene Compounding

MXene is a class of two-dimensional nanoscale transition metal carbides whose excellent metal conductivity, chemical stability, a high density of electron states and adjustable surface functional groups make them suitable for EMI shielding [135–138]. However, the poor mechanical properties of MXene materials lead to oxidation and degradation in humid environments, which in turn limits their effectiveness in applications requiring electromagnetic shielding [139–141].

Figure 7 depicts the fabrication process of MXene/wood composites and their electromagnetic shielding properties. Wei et al. applied MXene coating on both the tangential-section and cross-section of wood. They discovered that the impedance matching of the tangential-section was higher than the cross-section. This disparity was due to the unique pore structure of wood and the presence of free radicals (Fig. 7a) [142]. In addition, Wei et al. prepared MXene/wood composites by applying MXene on the wood surface and then coating it with self-crosslinking polyurethane-modified waterborne acrylic resin to achieve waterproof performance. Remarkably, the EMI SE of the

composite reached 31.1 dB [143]. The study broadens the application prospects of MXene/wood composites and solves the problem of oxidization and degradation in oxidization and degradation in humid environments. The spraying method is an expandable preparation technique applied to poplar, pine, and lychee wood. The EMI shielding requirements can be achieved commercially after 3–5 coats. Similarly, Cheng et al. employed UV-assisted chemical and mechanical spraying techniques to apply a coating of silver nanowires (AgNW) and MXene onto transparent wood. This process resulted in a sandwich composite material. They introduced structural shielding through a multilayer stacking method, leading to an EMI SE of 44 dB (Fig. 7b) [125]. In this case, the AgNW was sprayed on the MXene surface to enhance the electrical conductivity, and the ordered microtubule channel array of transparent wood induced multiple reflections of EMWs to enhance the EMI shielding performance [144].

Similarly, Jiang et al. prepared MXene/wood composites by immersing wood veneer boards with lignin removed by acid treatment into MXene suspension, which were hot-pressed into alternating multilayer structures, resulting in significant EMI shielding capability with an EMI SE of 32.7 dB (Fig. 7c) [145]. It is worth noting that as the MXene load increases, the EMI SE gradually increases. The EMI SE reaches its maximum when the load is 6.7 mg cm^{-3} . The experimental densification process enhances the flame retardancy and mechanical stability of the material and produces a dense conductive network that contributes to the absorption and reflection of EMW [146]. The surface of MXene/wood is noticeably smoother than natural wood, with MXene covering the narrow cracks. This MXene layer expedites electron transfer among neighboring MXene sheets, effectively creating a continuous conductive path.

Wang et al. developed a simple top-down method to transfer $d\text{-Ti}_3\text{C}_2\text{T}_x$ nanosheets onto cellulose scaffolds using vacuum pressure-assisted impregnation to make densely layered $d\text{-Ti}_3\text{C}_2\text{T}_x$ /cellulose scaffolds, which resulted in excellent mechanical and EMI shielding properties with an EMI SE of 39.3 dB [147]. The microstructure of $d\text{-Ti}_3\text{C}_2\text{T}_x$ /wood composites prepared in this experiment has an ordered laminar structure, which ensures the mechanical properties of the material and the reflection and absorption of battery waves. The pearly layered microstructure allows the remaining electromagnetic waves to combine with the high electron density

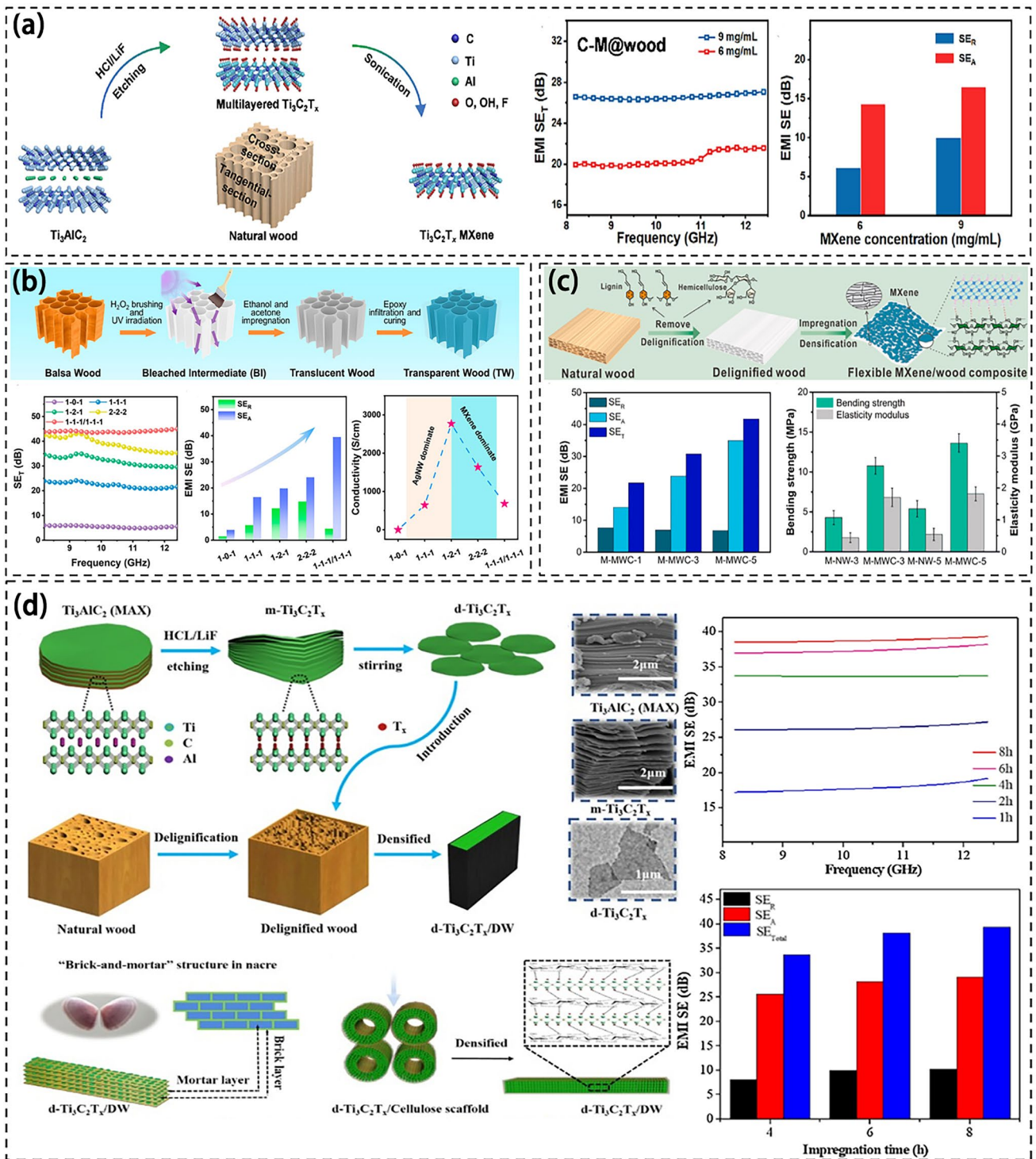


Fig. 7 a Preparation of highly anisotropic MXene@Wood composites and EMI shielding properties of cross sections [142]. b Illustration of the preparation process of WA-M/wood [125]. c Schematic diagram illustrating the fabrication for Flexible MXene/wood composite and EMI shielding performance of composite [145]. d Preparation and characterization of the d- $Ti_3C_2T_x$ /DW and EMI shielding performance of the d- $Ti_3C_2T_x$ /DW [147]

MXene layer and multiple internal reflections in the wood, allowing energy dissipation and absorption of EMWs [147, 148]. With the increase of impregnate time, the content of $d\text{-Ti}_3\text{C}_2\text{T}_x$ was escalated, and the corresponding EMI SE was also enhanced. The maximum shielding efficiencies of the $d\text{-Ti}_3\text{C}_2\text{T}_x$ /wood composites with diverse impregnate periods were higher than 99.95%.

MXene/wood composite methods are divided into two categories: impregnation method and spraying method. The primary objective of adding MXene to biomass materials is to create electric dipoles and interfacial polarization, thus affecting the propagation of EMWs. The EMI SE of the composites obtained is more than 30 dB, which meets the EMI shielding requirements of common industrial electronic instruments. The use of MXene composite offers a novel approach to creating electromagnetic shielding materials from biomass and opens up new possibilities for preparation methods. Research has demonstrated that MXene/wood composites can be tailored to meet specific property requirements, including mechanical strength, flame retardancy, flexibility, and transparency [149–151]. This advancement significantly broadens the potential applications of MXene/wood composites in EMI shielding, making them appropriate for application in extreme environments and presenting exciting opportunities for the future [152, 153].

The integration of MXene with wood is showing great promise for EMI shielding materials [154]. While MXene possesses remarkable conductivity and chemical stability, its poor mechanical properties in humid conditions pose a challenge. Various methods such as impregnation and spraying techniques, have been explored to address this limitation. The resulting MXene/wood composites have demonstrated significant EMI shielding capabilities exceeding 30 dB. These composites possess ordered microstructures that improve mechanical stability and EMI SE through electromagnetic wave reflection, absorption, and multiple internal reflections. Customizing MXene/wood composites may offer flexibility in meeting specific property requirements and expanding their potential applications across various industries [155].

3.1.2 Metal Compounding

Figure 8a–d shows the wood/metal composite preparation process and the EMI SE under different conditions. Pan

et al. developed a composite material with highly effective EMI shielding properties by creating a sandwich structure on wood with a nickel-plated surface. The material demonstrated an impressive absorption efficiency of 94.1 dB for EMI shielding which could be attributed to the synergistic impact of surface absorption loss and interfacial polarization loss [156]. When the coating is applied, the composite surface becomes smoother as it tightly integrates the Ni layer with the wood, resulting in a dense composite coating. This coating not only creates an effective conductive network but also enhances the hydrophobic properties of the composite material. Based on the loss mechanism, the Ni/wood composites leverage interfacial polarization loss, conductivity loss, and magnetic loss to absorb incident EMW [46]. However, a relatively large Ni layer thickness is required for better electromagnetic shielding properties. Therefore, it affects the degree of coating uniformity and manufacturing cost.

In addition, Pan et al. used electroless Cu plating to deposit Cu particles on the surface of poplar pasteboards to prepare laminated laminar composites. These composites exhibit absorption-based and reflection-based shielding mechanisms, providing an EMI SE of 96 dB and good hydrophobicity [157]. The multi-interfacial polarization within Cu and wood and the anisotropic internal porous structure of the wood matrix gives the prepared composites excellent EMI shielding properties [158]. As the duration of electroless Cu plating increases, the wood surface texture becomes smooth and the uneven pores are covered by metal particles, creating a consistent metal layer that forms a reliable conductive network. The presence of numerous interfaces between adjacent conductive networks such as air-Cu, Cu-Cu, and Cu-wood, leads to the absorption of incident EMW through multiple reflections [50, 159]. Additionally, the difference in dielectric constants results in the accumulation of free charge at the non-uniform interface boundary among metallic copper and wood, causing interfacial polarization and the generation of macroscopic dipole moments and Debye relaxation. This ultimately leads to the attenuation of EMW energy [160, 161].

Guo et al. conducted electroless Cu-Ni plating on wood surfaces. Firstly, Cu was deposited onto the wood, resulting in some Cu particles in the activation holes and on the wood surface. Subsequently, a Ni layer was applied to the Cu layer through electroless Ni plating, followed by the deposition of electroless Cu plating on the Ni layer. This process led to the creation of Cu-Ni multilayered composites with an

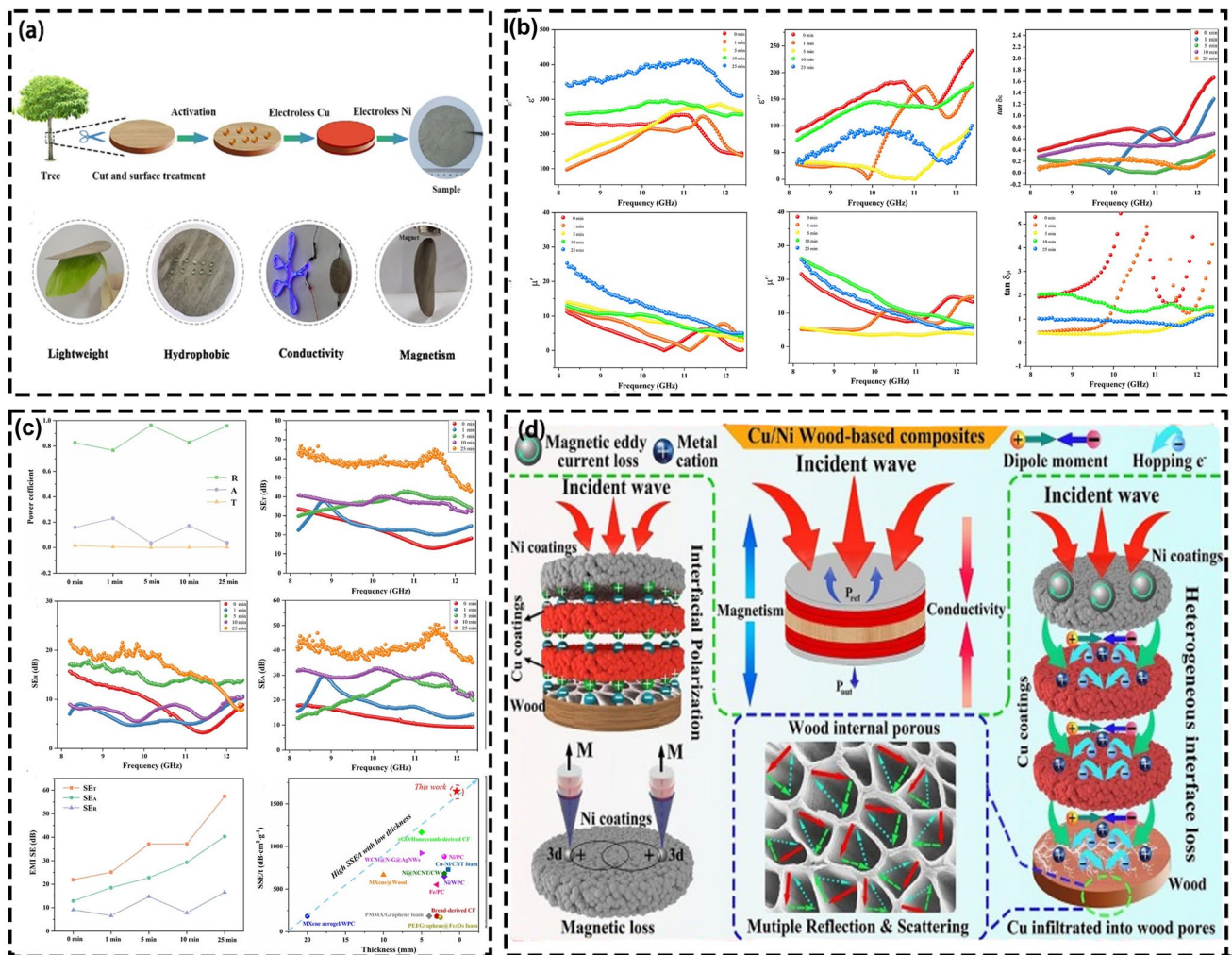


Fig. 8 Sandwich-structured Cu-Ni wood-based composites. **a** Preparation of Cu-Ni wood-based composites; **b** Electromagnetic parameters, magnetic loss tangent and dielectric loss tangent of each sample; **c** EMI shielding properties of sandwich-structured Cu-Ni wood-based composites; **d** Schematic illustration of absorption mechanism of Cu-Ni wood-based composites [164]

exceptional EMI SE of 93.8 dB. These composites exhibited impressive EMI shielding properties, favorable surface roughness, hydrophobicity, and electrical conductivity [162]. The fine Cu particles can fill the porous structure and surface defects of the wood, promoting the formation of a uniform metal layer on the wood surface. At the same time, the uniform Cu layer provides an autocatalytic substrate for the Ni particles deposition. The Cu and Ni layers on the wood act synergistically for electromagnetic shielding due to the conductive networks and the specific interfacial polarization mechanism of the composite coating and promote the absorption of incident EMW via the polarization of the electric field [163]. Furthermore, Dai et al. prepared a

Cu-Ni wood sandwich structure composite with an EMI SE of 57.4 dB by electroless copper-nickel plating. The composite formed a three-dimensional electromagnetic network and possessed an ideal microchannel structure with the copper-nickel coating (Fig. 8) [164]. It was found that the Ni and Cu nanoparticles within the composites form a network that facilitates electron movement, thus decreasing resistivity. The multiple non-uniform interfaces within the Cu, Ni, and wood and Ni layers and air also contribute to interfacial polarization [46].

Electroless plating is the primary method for laminating metal particles with wood, leveraging the abundant pores of wood to infuse metal particles and create a uniform metal

layer on the surface. Copper (Cu) and nickel (Ni) are commonly used metal particles. The integration of metal particles into biomass materials significantly enhances magnetic loss and EMW absorption capabilities while also improving electrical conductivity, impedance matching, and interface polarization within the composite [165]. The combination of wood-metal complexes with their porous wood structure and interfacial polarization facilitated by the metal layer exceeds commercial EMI shielding requirements with over 90 dB. This exceptional shielding effectiveness not only meets but surpasses the strict demands of sensitive instruments for

EMI shielding, representing a significant advancement in the field.

3.1.3 Polymer Compounding

Figure 9 shows the polymer/wood composite preparation process and their respective EMI SE. Karteri et al. utilized camphor pine wood chips, polyethylene (PE) and graphene nanoparticles to make microspheres through a twin-screw extruder and thermally pressed them to produce

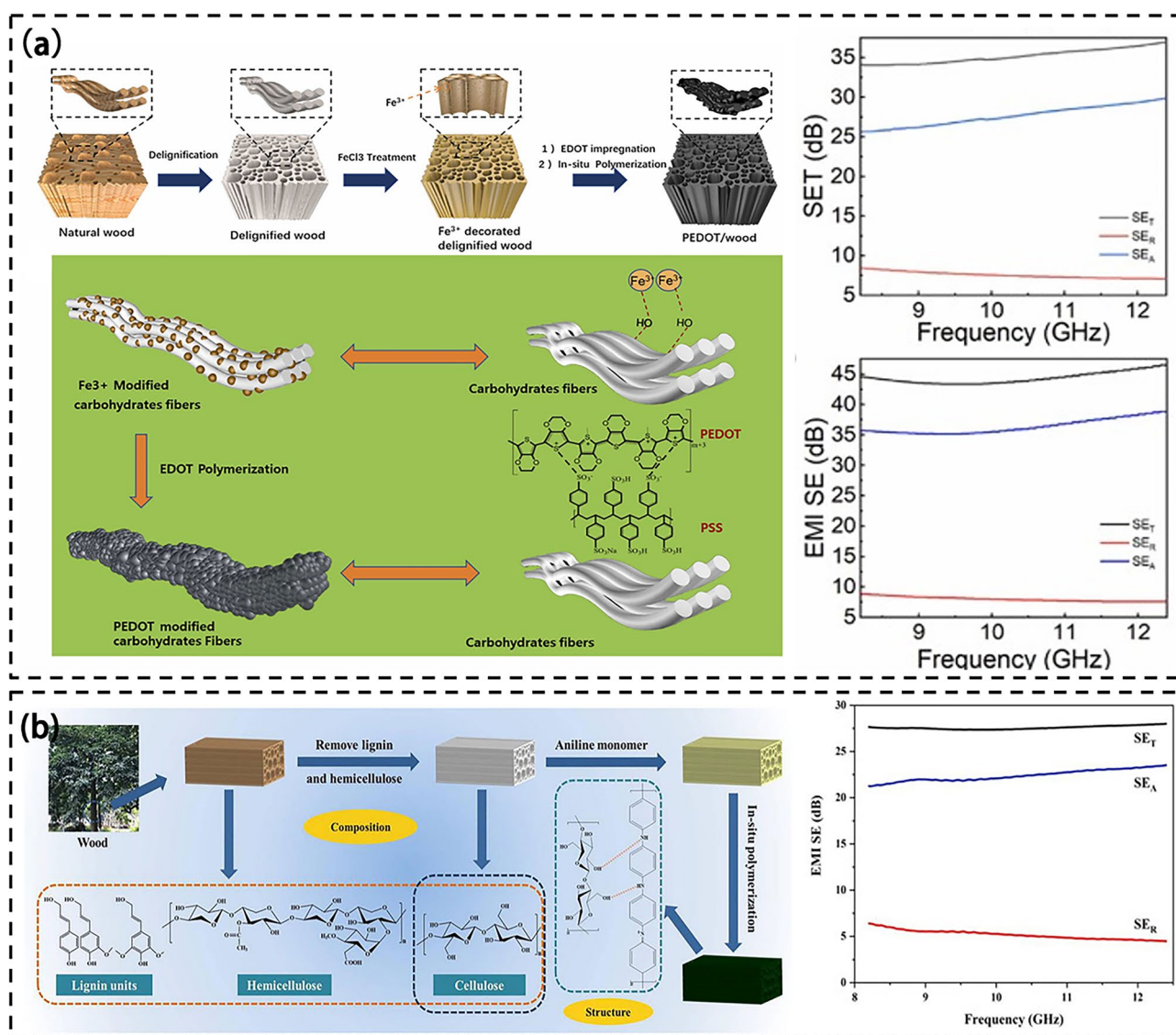


Fig. 9 a Scheme for preparing PEDOT/wood and EMI shielding performance of composite [167]; b Preparation process of PANI-WA aerogel and wood and EMI shielding performance of composite [168]

wood-polyvinyl chloride/graphene nanoflake nanocomposites with EMI SE of more than 25 dB [166]. This study demonstrates that a higher graphene content in the composite material reduces EMW penetration and enhances shielding efficiency. Specifically, the composite containing 9 wt% graphene exhibits superior EMI shielding performance, with a higher EMW absorption than reflection. This indicates that the material functions as an absorption-based EMI shielding material. In addition, Chen et al. used an in-situ polymerization method to eliminate lignin from wood by chlorination. Then, the monomers were coated on the carbohydrate framework of the delignified wood surface for in-situ polymerization to produce a polythiophene (PT)/wood composite with an EMI SE of 46 dB (Fig. 9a) [167]. The conductive network formed by PT in wood constitutes a continuous current pathway and the conductivity of the composite increases with increasing the mass fraction of thiophene. The shielding effect of its composites is mainly absorption, accounting for 80% of the total shielding effectiveness [158]. Additionally, the material has significantly enhanced mechanical properties, including a compressive strength of 50.9 MPa and a tensile strength of 67.8 MPa.

Additionally, Chen et al. have formed a non-carbonized nanostructured polyaniline (PANI)/wood composite with a 2–3 mm thickness, achieving an impressive EMI SE of 27.63 dB (Fig. 9b) [168]. PANI has an exclusive doping/dedoping and REDOX chemical structure that allows it to transition between insulating and conducting states and attach or detach various anionic groups [169]. This unique property can be harnessed to make wood electrically conductive. Delignified wood was coated with polypyrrole (PPy) via an in situ chemical vapor deposition as reported by Gan et al. The resulting product exhibited a tensile strength of 20.18 MPa and an EMI SE of 21–28 dB. However, the prepared composite has a low mechanical strength and a large thickness, which greatly limits its applicability.

Currently, the predominant method for fabricating wood-plastic electromagnetic shielding composites is in-situ polymerization. The resulting composites rely on electromagnetic wave absorption to achieve effective electromagnetic shielding performance. This is achieved by adjusting the dielectric properties of the polymer to ensure favorable impedance matching with air. Furthermore, the incorporation of conductive fillers facilitates the conductive network formation, thereby enhancing the EMI shielding performance of the material. This approach allows

efficient reflection and absorption of EMW, consequently reducing their penetration. However, challenges like low mechanical strength and substantial thickness impose limitations on its practical application.

3.1.4 Modified Adhesive

Figure 10a shows the principle that plywood can be used for electromagnetic shielding. Ma et al. found that by constructing microporous structure and isolation structure simultaneously, the material can have excellent EMI shielding performance based on absorption [170]. Xu et al. combined antibacterial agent quaternary ammonium salted hyperbranched polyamide (QHBPA) with graphene nanosheets (GNSs) to obtain G-co-Q hybrid [171]. The organic and inorganic hybrid plywood adhesive was prepared by electrostatic interaction and hydrogen bonding with soybean protein isolate (SPI) and phytic acid (PA). It not only shows the electromagnetic shielding performance of 43 dB, but also has good flame retardancy and mold resistance. A conductive layer isolated from each other is formed in the plywood through the adhesive, and the thickness of the conductive layer can be controlled by adjusting the thickness of the veneer to achieve better EMI SE. Among them, GNS is the main reason for its EMI shielding performance. Adjusting the concentration of G-co-Q hybrid ensures the mechanical strength and electromagnetic shielding performance of the plywood, among which, the adhesive containing 7.5% concentration of G-co-Q hybrid has the best performance (Fig. 10b). Similarly, Zhang et al. used dichloromethane, methacrylate anhydride (MA) to modify SPI, and grafted pyrrole (PY) and dopamine hydrochloride (DOPA) on SPI [172]. Ag NPs is generated locally in the adhesive and combined with self-synthesized biological crosslinkers to form hybrid adhesives. Among them, the addition of conductive polymer is the main reason for electromagnetic shielding, when adding 20 wt% PY adhesive, its conductivity can reach 7.09 S cm^{-1} , SET is 24.05 dB (Fig. 10c).

There is little research on adhesives that can be used in EMI shielding field. It is mainly the addition of highly conductive polymers to improve the conductivity, so as to meet the commercial requirements of EMI shielding. At present, further exploration of adhesives is still needed to provide better help for plywood in the field of EMI shielding.

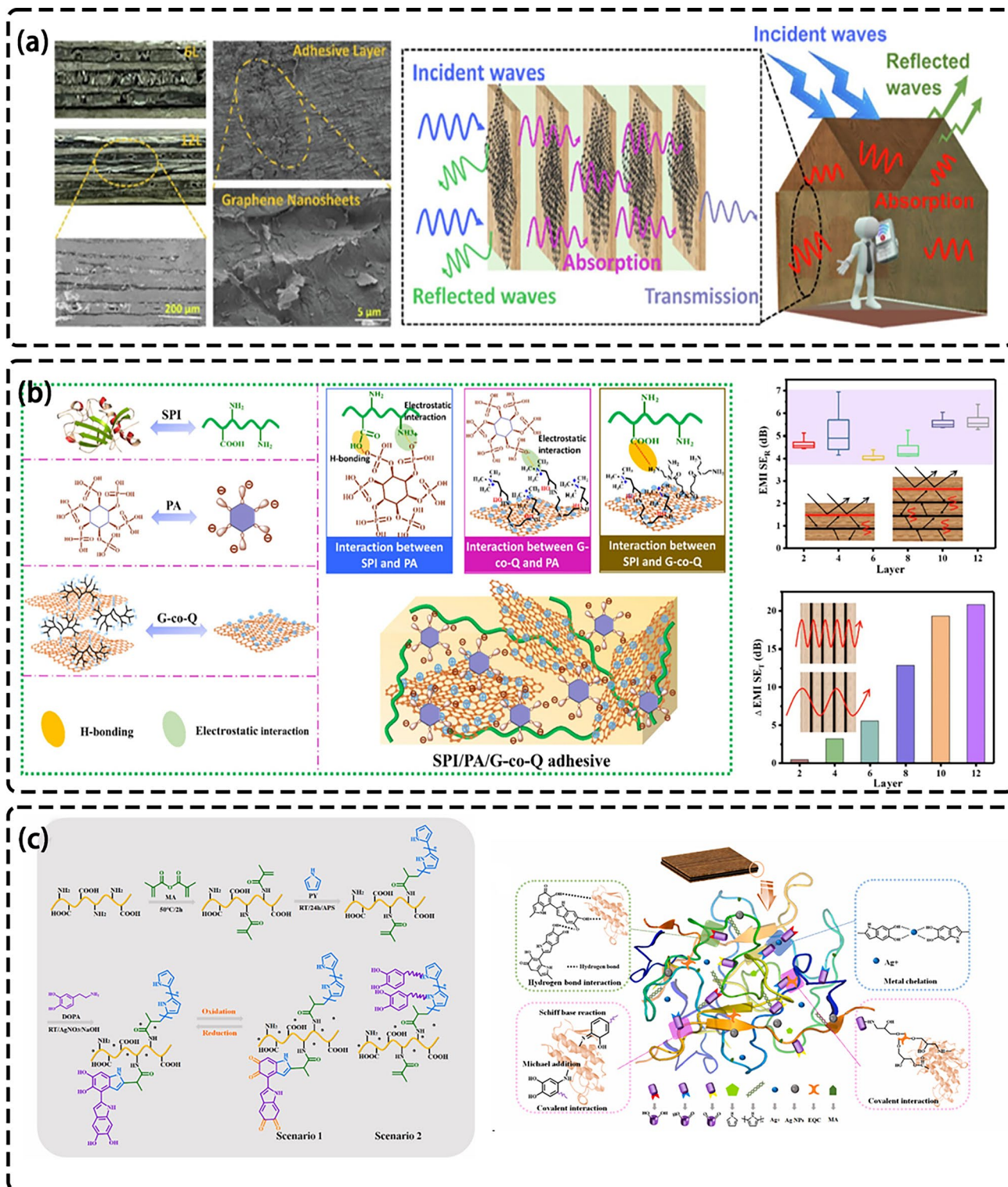


Fig. 10 a Principle of plywood for electromagnetic shielding [171]. b Preparation of organic-inorganic hybrid structures in protein adhesives and EMI shielding properties [171]. c Schematic diagram of preparation of strong conductive soybean protein adhesive [172]

3.2 Cellulose and Its Derivatives

Cellulose represents the most widely distributed and the largest reserves of natural polymer materials [173–176]. Cellulose has the advantages of being easily functionalized [177–182], exceptional biocompatibility, environmental friendliness, renewability, and biodegradability [183–185]. It can be easily processed in aqueous solutions, making it a highly versatile and sustainable material with broad applications in various industries [186–192].

Figure 10 shows the preparation process of cellulose composites and the effects of different concentrations on EMI SE. Li et al. prepared lightweight EMI shielding cellulose foam/carbon fiber composite material with SE of 60 dB by freeze-drying method [193]. The orientation of fibrous packing within the cell wall of bubbles is influenced by the significant tensile flow that occurs during the growth of the bubble. This flow promotes fiber enrichment and alignment, resulting in a tightly packed foam composite. As the volume expands, the distance between adjacent fibers increases. The short carbon fibers are positioned in the cellulose layer between the bubbles while the long carbon fibers can penetrate the bubbles, thus enhancing their electrical conductivity. Moreover, Lee et al. prepared a layered silver nanowire (AgNW) coated cellulose paper with an EMI SE of 48.6 dB via dip plating (Fig. 11a) [194, 195]. The cellulose fibers in AgNW/cellulose paper are randomly and uniformly coated with interconnected AgNWs. The cellulose paper interior contains AgNWs, forming a continuous conductive network [196]. The exceptional electrical conductivity of AgNWs contributes to the conductive network formation within cellulose paper. As a result, the composite material demonstrates excellent electromagnetic shielding capabilities [197]. Zhu et al. impregnated AgNWs into a highly arranged cellulose scaffold to produce a maximum tensile strength of 511.8 MPa, and an EMI SE of 46 dB [198]. The hydrogen bond between cellulose fibres and AgNWs creates a continuous conductive pathway within the CS microchannel. Through hot-pressing densification, nanofiber alignment is improved, and a more tightly packed conductive network is formed. As a result, this increases dielectric and reflection loss, ultimately enhancing EMI shielding performance (Fig. 11b). Similarly, Xu successfully prepared an efficient EMI shielding film by self-polymerization on CNFs through oxidation of dopamine (DA) and chemical

deposition of silver nanoparticles (AgNPs) on CNFs by pressure extrusion process. The resulting composite film has a tightly connected conductive network, which significantly improves the overall conductivity of the EMI shielding film and makes its EMI SE reach 93.8 dB [199].

In addition, Cui et al. created a lightweight composite membrane by combining MXene and CNF using freeze-drying and vacuum filtration techniques. The resulting membrane exhibited excellent mechanical properties, high electrical conductivity, and a highly porous structure, with an EMI SE of 53.7 dB [200]. The CNF was linked with MXene nanosheets through hydrogen bonding, creating a continuous conductive network structure and enhancing the mechanical properties of the composite film [201, 202]. The MXene/CNF composite film demonstrated high conductivity and abundant free charges on its surface, which effectively reflected most of EMW on its surface. As EMW entered the film, it interacted with the high-density charge in MXene while passing through its lattice structure, resulting in ohmic loss and a significant reduction in EMW energy. The porous structure of the composite film expedites multiple reflections of EMW, thereby promoting rapid absorption and attenuation of EMW [203, 204]. Similarly, Zhou et al. achieved an EMI SE of 60 dB by coating MXene on BC nanofiber film using repeated spraying and subsequently resulting in a dense layered nanocellulose film (Fig. 11c) [205]. Using chitin and aramid pulp as raw materials, Zhang et al. prepared chitin cross-linked aramid nanofibers (CANFs) by a room temperature synchronous deprotonation-protonation method, and combined with cross-linked chitin to prepare nanocellulose aerogel (CA). Finally, it was soaked in MXene suspension under vacuum to obtain a uniform porous structure. CA-M aerogel with low thermal conductivity ($0.01 \text{ W m}^{-1} \text{ K}^{-1}$) and high EMI SE (75 dB) [206].

Overall, cellulose-based materials for electromagnetic shielding are primarily produced using freeze-drying and dipping methods, resulting in composites with impressive electromagnetic shielding performance. The inherent interfacial polarization in cellulose-based materials enhances EMW loss while the addition of conductive fillers helps the charge distribution and enhances dielectric loss. Additionally, the natural porosity and abundance of hydroxyl groups in cellulose give it strong electrical conductivity, facilitating multiple internal reflections of EMW and improving EMI shielding performance [207]. Through hydrogen bonding, these materials can also achieve excellent mechanical



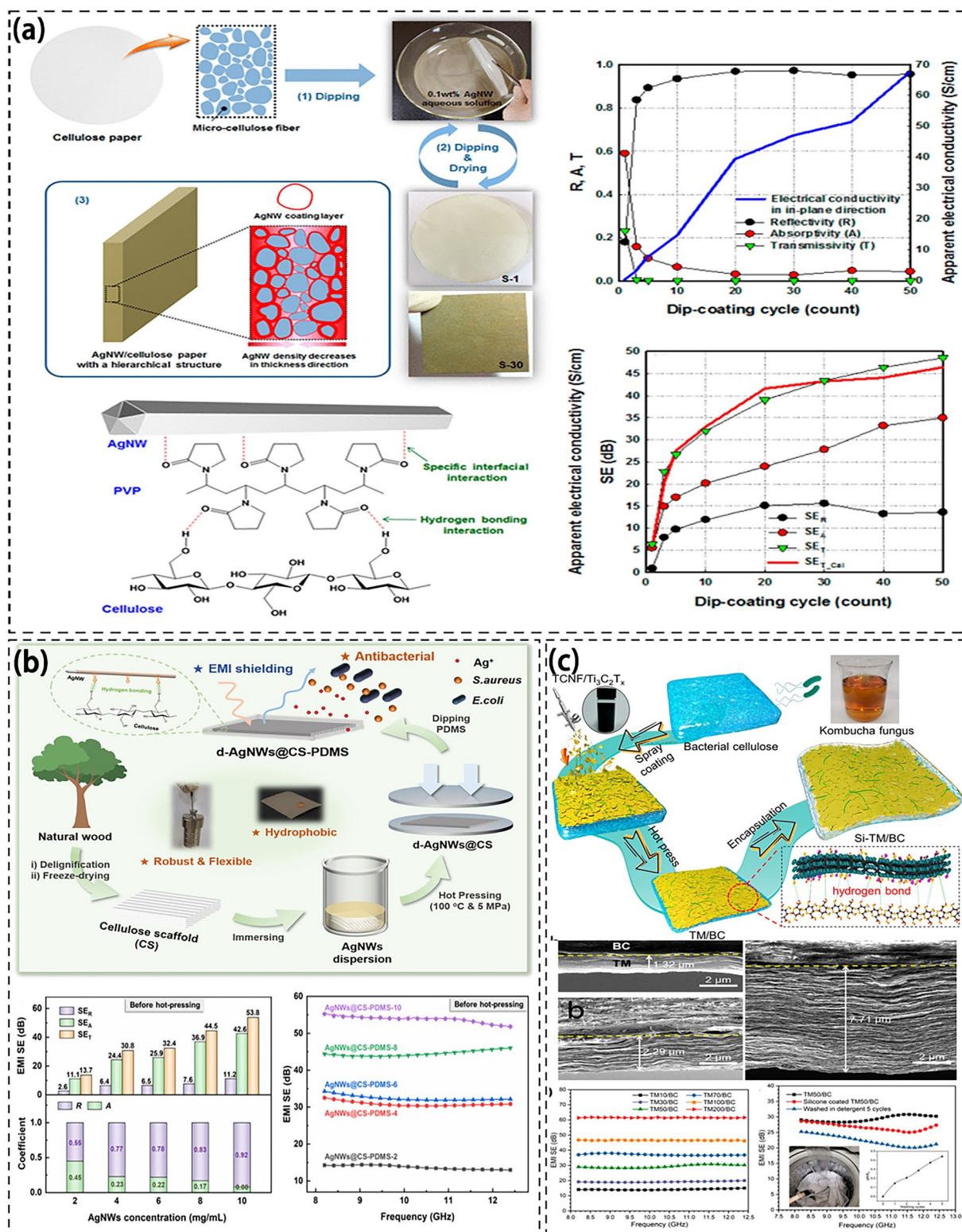


Fig. 11 a Schematic illustration of the creation process of the composite foams, the foam structure, and EMI shielding performance of composite [194]; b Preparation and EMI shielding properties of silver nanowire/aligned cellulose scaffold composite [198]; c Synthesis of Ti₃C₂ MXene/nanocellulose composite films [205]

properties and a continuous conductive network structure, rendering them appropriate for a wider utilization.

3.3 Lignin and Its Derivatives

Lignin is a green and renewable biomass material known for its degradability, stability, and low costs [208, 209]. Lignin possesses a porous structure and a complex carbon skeleton structure with numerous benzene rings that contribute to its EMI shielding performance [210, 211]. Additionally, its porous surface is abundant with active sites and functional groups such as free hydroxyl and carboxyl [212], hence allowing it to undergo various chemical reactions with other materials [213–216]. These exceptional chemical properties make lignin an encouraging option for EMI shielding applications.

Figure 12 illustrates the preparation process of lignin composites and the effect of different concentrations on EMI SE. Zhang et al. used an in-situ insertion method to synthesize lignin-based polyurethanes from graphite, hexamethylene diisocyanate, polyethylene glycol and modified reduced iron powder with lignin. The composite material with 10% iron and graphite content plus 20% lignin content achieved an EMI SE of 22.5 dB [217]. This material exhibits excellent electromagnetic shielding properties, strong mechanical properties, and high thermal stability. It was found that the presence of the phenyl group in lignin creates an opposing magnetic field that shifts and shields the EMW. Additionally, the material can form π bonds with the graphite to enhance the uniform distribution of graphite in the matrix, thereby improving the shielding effectiveness. Then, the evenly distributed iron, graphite, and polyurethane matrix also interact strongly to yield a synergistic effect. However, higher iron and graphite content led to reduced tensile and fracture strength, as well as a rougher surface which negatively impacted the filler-matrix interface [218].

Hu et al. synthesized lignin-based polyurethane by in-situ synthesis of modified Fe_3O_4 , modified CNT, polyethylene glycol and hexamethylene diisocyanate. When the composite contains 10% Fe_3O_4 , 10% CNTs, and 15% lignin, it exhibits an EMI SE of 37.51 dB [210]. The presence of Fe_3O_4 facilitates electron hopping and results in high electrical conductivity in composites. Moreover, the composites demonstrate magnetic loss properties, abundant interfacial polarization, and a well-assembled conductive carbon nanotube network,

facilitating efficient absorption, scattering, and reflection of incident radiation. The inclusion of lignin molecules induces a three-dimensional network structure formation with CNTs and Fe_3O_4 , thereby extending EMW propagation and creating multiple reflection paths within the composites [219]. Additionally, the uniform distribution of CNTs and Fe_3O_4 within the polyurethane matrix forms an excellent conductive network, further enhancing electromagnetic shielding effectiveness. Overall, the combined effect of Fe_3O_4 , CNTs, and lignin significantly enhances the EMI shielding performance of the composite.

Besides, Zhang et al. employed the freeze-drying technique to create a sandwich structure composite with a lignin-based epoxy acrylic ester. The freeze-drying method was used to obtain an intermediate layer by the in-situ reaction of lignin, epoxy resin, acrylic ester, modified Fe_3O_4 nanoparticles, and multi-walled CNTs. A 0.5 mm lignin-based epoxy acrylic ester coating was applied on both sides to produce the composite. Notably, when the Fe_3O_4 and multi-walled CNT content was at 5% and lignin at 15%, the composite demonstrated an EMI SE of 14.8 dB (Fig. 12a) [220]. The interaction between the benzene rings in lignin and the CNTs facilitates a uniform distribution of CNTs, forming an effective conductive network and improving electromagnetic wave reflection.

In addition, Zeng et al. employed a simple freeze-drying method to prepare a 2 mm thick composite aerogel made of lignin-derived carbon (LDC) and RGO. This aerogel demonstrated an EMI SE of 49.2 dB, featuring three-dimensional, micrometer-sized pores and unidirectional cell walls [126]. The molecular properties of lignin result in an interaction with GO that further leads to RGO/LDC aerogels with thinner, larger, and more cell walls. As a result of tightly packed cell walls, it possesses a larger effective reflective surface area and improves its multiple reflective properties (Fig. 12b). Overall, the combination of numerous reflection effects, high absorption capacity of the cell wall, and a significant number of carrier-induced electrical losses in the cell wall results in the RGO/LDC aerogels with excellent EMI SE at ultra-low density [221, 222]. Besides, Liu et al. incorporated fireproof polypropylene into lignin and combined it with MXene to create functional lignin nanoparticles. This composite material exhibits excellent fire resistance, superior electromagnetic shielding capabilities, and aging resistance (Fig. 12c) [223].

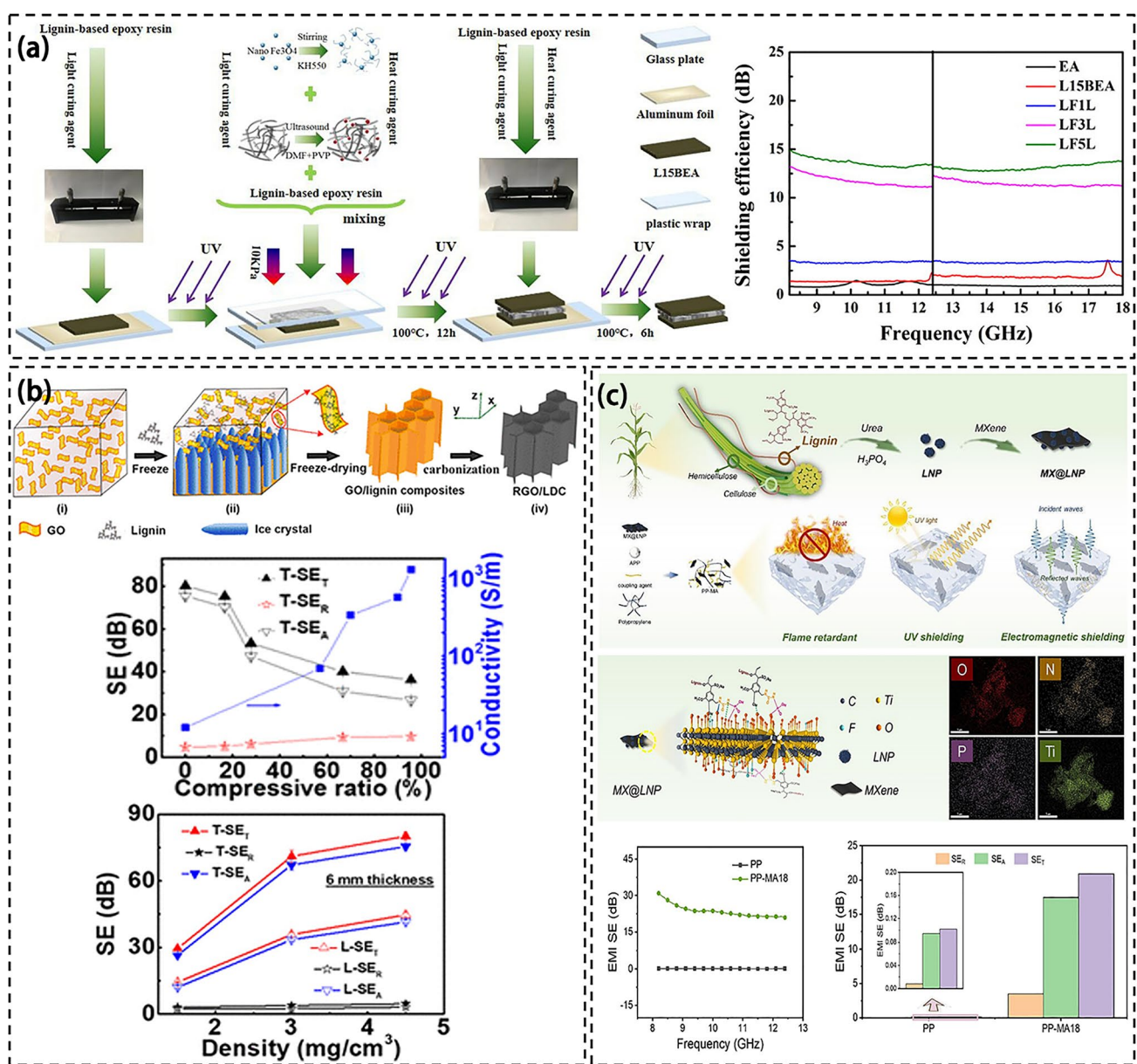


Fig. 12 a Preparation process of FCLBEA shielding material and EMI shielding performance of composite [220]. b Fabrication process of RGO/LDC aerogels and EMI shielding performance of RGO/LDC aerogels [126]. c Preparation of multifunctional lignin nanoparticles and their composite structures and electromagnetic shielding properties [223]

Currently, lignin processing methods are relatively simple and usually involve freeze-drying or in-situ polymerization. Electromagnetic shielding materials typically use Fe₃O₄, Fe, and CNT as fillers. By leveraging the porous structure and benzene skeleton of the lignin, Fe₃O₄ can regulate electron movement while CNT forms an effective conductive network. The combined effects of these components significantly enhance the EMI SE of the composite [218, 224].

3.4 Bamboo and Its Derivatives

Bamboo represents a green and renewable biomass material with abundant resources, lightweight, easy to process, low cost, short growth cycle and biodegradable [225–227]. Bamboo is composed of bamboo skin, interior and pulp, in which its structural composition may affect the conductivity of different parts [228].

Figure 13 shows the preparation process of bamboo composite materials and the influence of various proportions of concentrations on EMI SE. Zhang et al. performed

electroless Ni-Fe-P plating on bamboo fiber as the reinforcement phase. Then, the metallized bamboo fiber was incorporated into polylactic acid (PLA), followed by hot pressing.

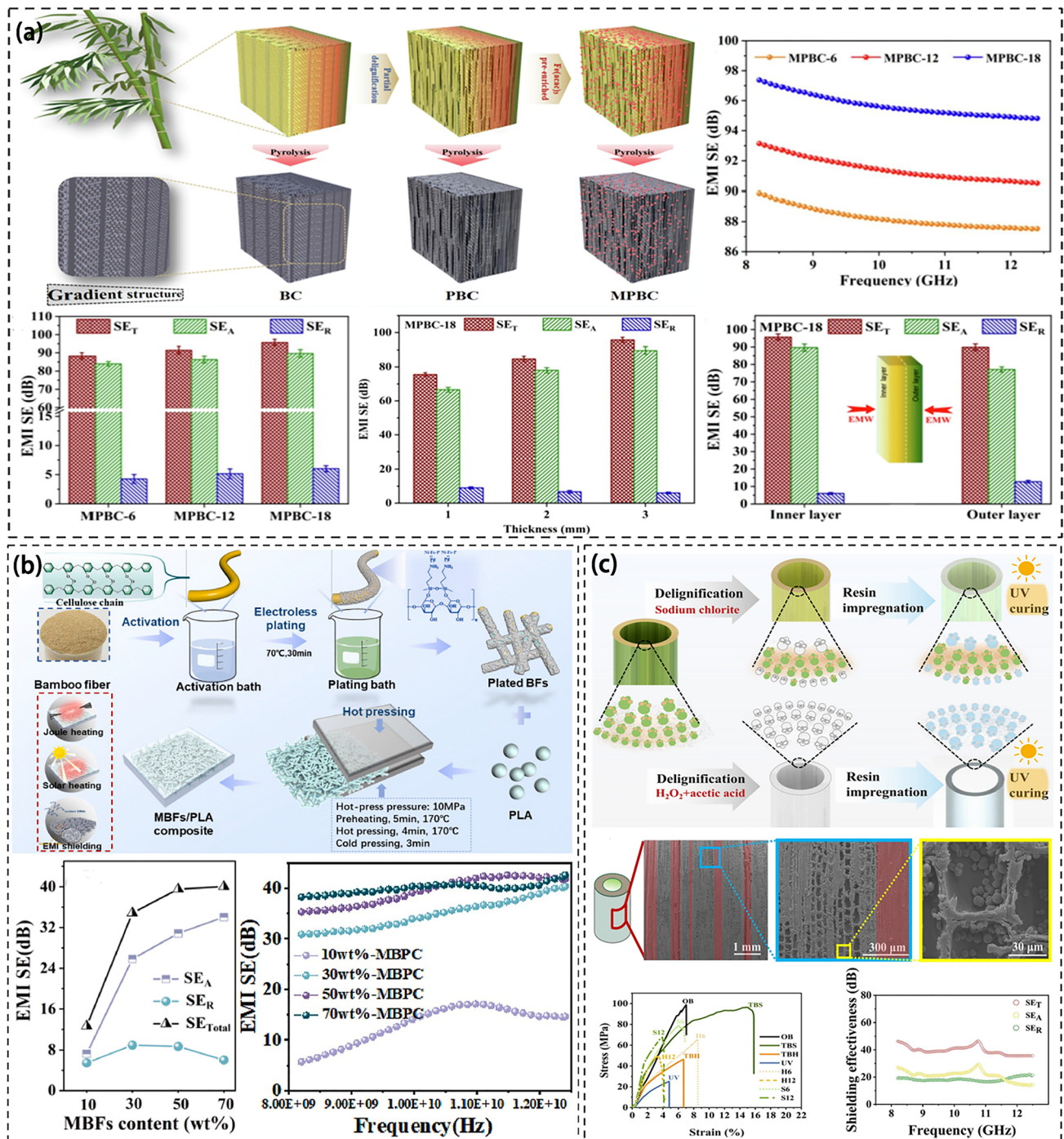


Fig. 13 a Fabrication process of MBF/PLA composite and EMI shielding performance of MBF/PLA composite [229]; b Process and principle of nickel activation and surface resistivity of bamboo outer peel, bamboo inner peel, and bamboo pulp [233]; c Preparation of transparent building bamboo and its mechanical properties and EMI shielding properties [235]

This resulted in the creation of a metallized bamboo fiber (MBF)/PLA bamboo matrix composite with an EMI SE of 45 dB (Fig. 13a) [229]. The PLA material effectively integrates with the metallized bamboo fiber (MBF) by forming a strong and compatible interface. As the filler content increases, the metal particles distribution on the bamboo becomes more uniform, and the conductive network is improved [230]. The overlapping of MBF within the PLA matrix creates a three-dimensional conductive network that enhances the scattering and electromagnetic losses of the MBF/PLA composite [231, 232]. The use of a higher bamboo fiber (BF) content results in more contact points between the fibers, leading to increased conductive paths and a complete conductive network. Additionally, the metal coating enhances the mechanical strength and thermal stability of the bamboo-based composite.

Zhang et al. coated bamboo with electroless Ni–Fe–P plating [233]. The metal particles are uniformly distributed on the bamboo surface and continuously form a dense conductive network to obtain a uniform and dense metal coating with the crystal structure. For the first time, they studied the difference in the surface conductivity of coated bamboo. The results revealed that bamboo shrinkage rates varied based on vascular bundle density. The adhesion of the metal coating to the bamboo skin was weak, which affected the conductive pathway continuity. Conversely, the metal coating on the bamboo pulp was uniform and dense [92, 234]. The different parts exhibit varying electrical conductivity, with the edge demonstrating higher conductivity than the middle part. This is attributed to the infiltration of metal elements in both the longitudinal and transverse planes (Fig. 13b).

In addition, Wang et al. prepared bamboo-derived carbon (BC) scaffolds with aligned microchannels, layered gradient and anisotropic as shielding materials by pyrolysis, with an EMI SE of 81.52 dB [195]. BC possesses numerous honeycomb pores, which are highly effective for absorbing and shielding EMW. The electrical conductivity of BC is affected by the annealing temperature. As the annealing temperature rises, the outer sheath of BC vascular bundles becomes denser and smoother, leading to increased contraction of vascular bundles and parenchyma, plus a decrease in the cell gap. This results in a reduction in disordered carbon and promotes more uniform grain growth and grain orientation. The abundant ionic motion in BC induces polarization, while the introduction of metal particles enhances electrical

conductivity. It was observed that treating BC with lignin increases the number of porous cracks on its surface. A crack-rich surface, gradient porous interior, and excellent conductivity facilitate superior EMW dissipation through multiple internal reflections, relaxation loss, and conductivity loss. Notably, Wang et al. modified bamboo by impregnating UV resin onto the fiber skeleton. This results in a building material with 60% light transmissivity, exceptional mechanical properties, and an EMI SE of 46.3 dB (Fig. 13c) [235].

In summary, electroless plating is primarily utilized in producing bamboo-based materials for electromagnetic shielding. This process capitalizes on the physiological properties of bamboo, resulting in anisotropy and varied conductivity. Bamboo-based composites are characterized by a rich cracked surface, porous interior, and dense conductive network. They also exhibit enhanced electromagnetic wave reflection, thereby achieving superior electromagnetic shielding performance [236].

3.5 Other Biomass Materials

Figure 14 shows the preparation process the composite materials and their respective EMI SE. Textile and fabrics have been used to prepare EMI shielding materials [237] and other electronics [238–242]. For example, Wang et al. used a hydrothermal reaction to remove lignin from sugarcane and annealed sugarcane (Fig. 14a). The sugarcane/graphene oxide (GO) hybrid foam was obtained by dipping the treated sugarcane into the GO suspension and filling the GO with vacuum-assisted impregnation. The EMI SE of the composite reached 53 dB when the GO content was 17 wt% [243]. The GO was found to be connected to sugarcane through hydrogen bonding and π - π bonding interactions to facilitate electron transfer. Sugarcane cell walls were grafted with many GO nanosheets to enhance the connection within neighboring cell walls and form more conductive pathways. The GO nanosheets were in a closer contact with the increase of GO loading and exhibited stronger electron transport ability. The composite material retains the natural porous structure of sugarcane where its porous structure and rich interfaces reflect and absorb a large amount of EMW, thus improving its EMI shielding performance.

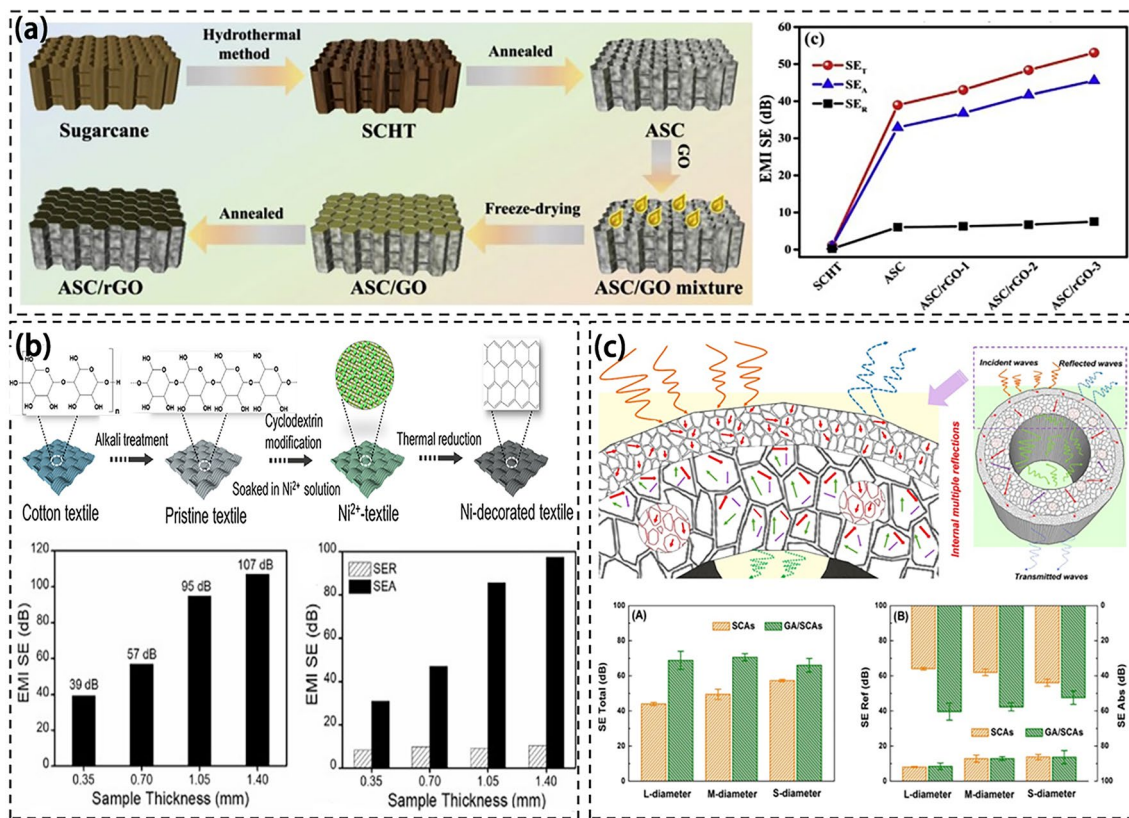


Fig. 14 **a** Fabrication process of ASC/RGO and EMI shielding performance of ASC/RGO composite [243]; **b** Schematic showing the fabrication process of Ni-decorated textile and EMI shielding performance of Ni-decorated textile [244]; **c** EMI shielding mechanism of straw-derived carbon and EMI shielding properties after modification [102]

In addition, Peng et al. used Ni as a catalyst to carbonize cotton at 900 °C to produce a textile with an EMI SE of 107 dB [244]. The high degree of graphitization of Ni-treated textiles produced the carbon with a high crystallization degree and a perfect six-membered grid structure, facilitating electron transfer. Ni-treated fabrics with interwoven conductive networks promote the conduction loss in which the dipole polarization is caused by local dipoles on the surface defects of carbon fiber and the end functional groups of affinity agents. The interface polarization is improved with the uniform distribution of Ni particles. Magnetic Ni provides excellent magnetic loss for textiles through eddy current loss, exchange resonance and natural resonance [245]. Multiple EMW scattering and reflections occurred in multilayer micro-structures and nano-structures. These characteristics give nickel-treated textiles excellent electromagnetic shielding properties (Fig. 14b).

Wheat straw has attracted interests [246, 247]. Ma et al. utilized wheat straw to create a structured assembly after carbonization (Fig. 14c). They incorporated ultra-light graphene aerogel into the hollow part of the assembly, resulting in the development of a new electromagnetic shielding material derived from straw. This material exhibits low density and an impressive EMI SE of 66.1 dB [102]. The orderly porous structure of the material allows for multiple EMW reflections within the layers, thereby enhancing its ability to absorb microwaves and ultimately improving its EMI shielding performance.

Existing studies highlight various approaches to fabricate composite materials with significant EMI SE. These methods include utilizing Ni catalysts for carbonization, KOH-activated straw carbon, integrating graphene aerogel into wheat straw, and forming sugarcane/GO hybrid foam. Each technique capitalizes on unique material properties

such as a high graphitization degree, porous structures, interconnected pathways, and bonding interactions to optimize electron transfer and enhance EMW absorption. The results emphasize the potential of tailored composite materials to effectively mitigate EMI, thus offering promising solutions across diverse applications [248]. However, cotton straw usually has a high porosity, and its high porosity leads to the leakage of EMWs. Cotton and hemp straw has a large volume, which may affect its use in applications with strict volume requirements such as portable devices. When used in combination with other materials or technologies, cotton and hemp straw still have compatibility issues and requires specific treatment or formulation to ensure shielding effectiveness.

4 Electromagnetic Shielding Performance and Application of Biomass Composite Materials

MXene/biomass composite materials exhibit impressive mechanical properties, exceptional flame retardancy, and strong electromagnetic shielding capabilities (Table 1). Furthermore, coating treatments can enhance their water and corrosion resistance, making them suitable for use in various challenging environments. These versatile composites find applications in communication, electronics, and residential (Fig. 15a–d). A metal layer is applied to their surfaces through complexation involving metal particles and biomass materials to create a dense conductive

Table 1 Conductivity, electromagnetic shielding properties and tensile properties of MXene/Biomass composite materials

MXene/Biomass	Tensile strength (MPa)	EMI SE (dB)	Conductivity ($S\ m^{-1}$)	Reference
AgNW@MXene/ South American balsa wood	47.8	44.9		[125]
MXene/Cellulose Nanofiber	65.0	53.7	24,875	[200]
WA@MXene/Poplar wood		31.1		[143]
MXene/Balsa wood	68.1	32.7	1858	[145]
MXene/wood-derived hierarchical cellulose scaffold		39.3	6333	[147]

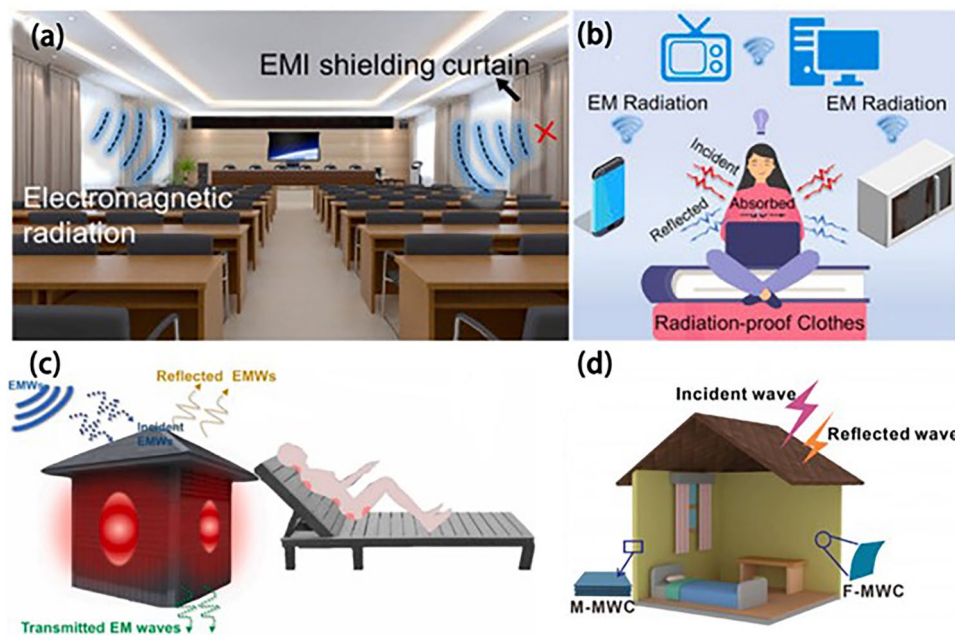


Fig. 15 Application of biomass EMI shielding materials in construction, furniture and clothing [145, 229, 244]

Table 2 Hydrophobicity, electromagnetic shielding properties and conductivity of composite materials

Metal/Bio-mass	Hydrophobicity	EMI SE (dB)	Conductivity ($S\ m^{-1}$)	Reference
Ni/wood/Ni	118.3°	94.1	16.60	[156]
Ni/Cu/wood	123.0°	93.8	29.54	[162]
Ni/wood-derived porous carbon		34.1	9.25	[46]
PLA/MBF		45.0	0.21	[229]
Fe ₃ O ₄ /Fe/BC		95.6	1238.93	[195]
Ni-Fe-P/bamboo	119.1°	55.0	4600	[233]

network. This results in significantly improved conductivity and electromagnetic shielding properties, which can be attributed to the abundant interfaces and porosity within the composite.

The metal/biomass material is combined to create a consistent metal layer on the surface with a dense conductive network [249]. This composite significantly improves conductivity and electromagnetic shielding properties due to its numerous interfaces and porosity (Table 2). The high hydrophobicity of the metal layer in the wood-based composite electromagnetic shielding material allows the multilayer composite to exhibit excellent hydrophobicity, making it suitable for humid environments. While bamboo-based composites shield slightly less than wood-based composites, they still meet industrial electronic instruments shielding requirements. Considering the unique arrangement of microchannels and superior conductivity of bamboo-based composites, they are well suited to energy storage, conversion, and multifunctional electromagnetic shielding [250]. In short, lignin-based composites are known for their favourable mechanical properties and heat stability, making them a popular option for various military and civilian applications.

Polymer/biomass materials are known for their relatively thin profile compared to other composites while exhibiting excellent mechanical and conductive properties (Table 3) [84]. These materials possess strong electromagnetic shielding properties that meet commercial use standards. They are frequently utilized in various applications, like electronics, military and civilian fields, robotics, communications, aviation, defense, scalable packaging, and construction materials [17, 251, 252].

Table 3 The conductivity, electromagnetic shielding properties and tensile properties of Polymer/Biomass composite materials

Polymer/Biomass	Tensile strength (MPa)	EMI SE (dB)	Conductivity ($S\ m^{-1}$)	Reference
PEDOT/wood	68.7	46.2	112.8	[167]
PANI/wood		27.6	22.07	[168]
CNT/PU/lignin	7.25	37.5	0.48	[212]
G/PU/lignin	11.7	22.5	0.01	[217]

5 Challenges and Prospects

Significant advancements have been achieved in biomass electromagnetic shielding composites in recent years. The growing interest in sustainable EMI shielding composites is attributed to their exceptional properties. However, a dearth of literature on biomass composites for EMI shielding impedes their further advancement. Owing to their remarkable hydrophobicity, flame retardancy and EMI shielding characteristics, these composite materials find potential applications in construction and furniture [253–256], aerospace [257], challenging environments [258, 259], and multifunctional EMI shielding [260, 261].

Biomass materials can improve their heat resistance through specific treatment and modification, and then maintain a good electromagnetic shielding effect in high temperature environment. The current research landscape in wood gilding predominantly revolves around an electroless nickel or copper plating on wood, with limited exploration of other metals and biomass materials. The EMI shielding and mechanical properties of biomass composites can be enhanced by combining various metals with biomass materials such as silver, aluminum, and iron. In addition, it has a certain impact on the flame-retardant performance of wood, such as adding iron particles, which can catalyze the formation of carbon layers in the combustion process of wood and slow down the combustion inside the wood. Some metal particles may also form a protective layer of metal oxide on the surface of the wood to achieve flame retardant effect. The existing methods for synthesizing wood composites are complex and time-consuming. Furthermore, the poor interfacial compatibility of wood with other materials coupled with its inherent defects including anisotropic and inhomogeneous characteristics, wet swelling, dry shrinkage,



and susceptibility to corrosion, could significantly impact electromagnetic shielding performance [168, 262]. As such, prospective research endeavors could commence with chemical modification and surface treatment of wood to obtain a uniform surface coating and a dense conductive network (Fig. 16).

Most treatment methods for cellulose materials are focused on surface treatment or modification, with a particular attention to the impact of three-dimensional pores on electromagnetic shielding. The resulting composite exhibits favorable mechanical properties and lightweight characteristics and significantly surpasses commercial requirements for EMI SE. However, limited research has been conducted on its waterproofing, heat resistance, and mildew resistance properties. This makes it impossible to use in wearable, portable designs. Cellulose materials can be used to construct multifunctional EMI shielding materials with flame retardancy by in-situ polymerization and coating technology. In addition, by combining with other nano-fillers, such as metal nanoparticles, not only the EMI SE can be improved, but also the flame retardant performance can be enhanced. The flame retardant properties of cellulose-based materials can improve the safety of electromagnetic shielding materials, especially in environments with dense electronic

devices and high power applications. Moreover, it can have a wider application potential in aerospace, military equipment, electronic products and other fields with high safety requirements. Future developments in cellulose materials should prioritize performance optimization to ensure reliable functionality under challenging environmental conditions.

Lignin-based composites may exhibit diminished mechanical properties in terms of elongation at break and reduced tensile strength, which could be attributed to metallic elements and graphite. Consequently, the EMI SE of these composites is inferior to that of their wood-based counterparts, with some failing to meet commercialization standards. In order to enhance their electromagnetic shielding performance, the composites have been augmented with fillers such as Fe_3O_4 , Fe, G, and CNT. Optimal electromagnetic shielding could be achieved by adjusting the lignin, iron powder, and graphite ratios. Nonetheless, these studies overlooked flame retardancy, hydrophobicity, and mildew resistance [212]. In order to overcome these constraints, forthcoming research endeavors should prioritize enhancements in the mechanical properties of composites, the chemical modification of lignin to instill advantageous chemical attributes, and the expansion of potential applications for lignin-based composites.

The heterogeneous physiological structure of bamboo results in varying coating thickness across its parts, leading to differences in resistivity and shielding effectiveness [263]. For future research endeavors, it is recommended that bamboo undergoes pretreatment to mitigate the influence of its structure on its functionality. This may involve acid treatment, alkali treatment, and physical modification to improve the mechanical and physical properties of bamboo, enhance dimensional stability, and augment its compatibility with the polymer matrix [264, 265].

In addition, future research in biomass composites should be on developing multifunctional biomass EMI shielding composites that can be effectively utilized in practical applications. It is essential that these composites not only exhibit outstanding electromagnetic shielding properties but also demonstrate remarkable environmental adaptability, including weather resistance, Flame retardancy, corrosion resistance, and waterproof properties. There is still significant potential for innovation and advancement in the research of biomass EMI shielding composites, particularly in enhancing electromagnetic shielding materials to be lightweight and thin, while possessing multifunctional attributes.



Fig. 16 Composite direction, properties, characteristics and applications of biomass EMI shielding materials in the future [229]

6 Conclusions

The increasing prevalence of electromagnetic pollution posits a considerable intimidation to information security, ecosystems and human health. As environmental consciousness grows, and resources are increasingly depleted, traditional electromagnetic shielding materials have revealed their inherent limitations in research and production. Consequently, the development of environmentally friendly and sustainable EMI shielding materials is crucial for safeguarding electronic equipment, preventing information leakage, and protecting public health.

This paper summarizes recent developments in biomass EMI shielding composites, including the underlying mechanisms of EMI shielding, the applications of various types of biomass EMI shielding materials, and the preparation methods for biomass EMI shielding composites such as coating, impregnation, in-situ polymerization, in-situ insertion, and chemical plating. Mainstream processing methods namely MXene composite and chemical plating, have been instrumental in enhancing the shielding performance, mechanical properties, and flame retardant capabilities of these composites. Additionally, modifications to biomass materials have induced desirable properties such as transparency, waterproofing, and mildew resistance, thereby expanding the potential applications of biomass materials in electromagnetic shielding. Despite these advancements, research on biomass EMI shielding composite materials remains relatively limited compared to other materials. Several unresolved issues persist involving inherent defects in biomass materials, anisotropy, varying electrical conductivities in different parts, corrosiveness, single functionality, and the non-waterproof nature of biomass materials.

1. *Diversity of materials* Biomass materials are limited for EMI shielding, with wood being the primary raw material for modification and relatively simple reagents being used for the modification process. However, certain wood properties, such as corrosion resistance, heat resistance, and hydrophobicity, do not meet the requirements. Additionally, wood modification often produces toxic gases. Therefore, it is essential to comprehensively compare various biomass materials and select those that meet the requirements for modification or composite. This approach can significantly reduce production costs and environmental pollution. The use of different fillers for treatment may yield varying effects such as the pro-

duction of transparent wood resistant to EMI and bamboo with uniform inner and outer layer properties. By comparing a range of biomass materials, it is feasible to obtain satisfactory chemical and mechanical properties that meet commercial standards. Thus, increasing the diversity of biomass materials is crucial as it creates electromagnetic shielding materials with special properties through modification or composite production to address the specific needs of consumers.

2. *Net zero emissions* In the production process of biomass materials, it is imperative to consider the modification of different fillers as it can release harmful gases. These harmful gases can be reduced by simplifying the experimental steps or reselecting the appropriate fillers. It is also crucial to assess the potential generation of greenhouse gases throughout the entire life cycle including the source, production, sales, and recycling stages to devise promising strategies for emission reduction. A comprehensive life cycle approach could be established to achieve zero carbon emissions. In order to meet commercial requirements, efforts should be made to improve production efficiency, ensure pollution-free production, facilitate convenient recycling, and further reduce greenhouse gas emissions and environmental pollution.
3. *Machine learning* Through the analysis and research of biomass materials, various fillers can be analyzed through artificial intelligence (AI) technology to improve the performance of biomass materials and improve one or more mechanical or chemical properties. Through machine learning, more suitable preparation processes or equipment can be selected to meet the high efficiency, safety and reliability of production. Through machine learning and AI technology, the performance and production efficiency of materials can be greatly improved, and the danger of experiments can be avoided, and environmental pollution and greenhouse gas emissions can be reduced.
4. *Circular economy* The utilization of biomass materials as the primary components for electromagnetic shielding materials offers several advantages. These materials are readily available from natural sources and can be extricated from wastepaper or other products, hence providing sustainable secondary uses. From a life cycle perspective, this approach significantly extends the lifespan of the materials and reduces waste. Waste can be recycled multiple times for pulp molding or padding and subsequently for versatile applications. Maximizing the utilization of biomass materials across the entire lifecycle, from sourcing and production to sales and recycling, a high raw material utilization rate can be achieved to



increase natural recycling, thereby mitigating environmental impact.

Acknowledgements The authors thank the National Natural Science Foundation of China (32201491), Young Elite Scientists Sponsorship Program by CAST (2023QNRC001). The authors extend their appreciation to the Deanship of Scientific Research at Northern Border University, Arar, KSA for funding this research work through the project number “NBU-FPEJ-2024-1101-02”.

Author Contributions Yang Shi and Mingjun Wu: Data curation, Writing—original draft, Validation, Investigation, Formal analysis. Shengbo Ge: Writing—original draft, Conceptualization. Jianzhang Li: Supervision, Methodology, Resources, Project administration, Funding acquisition. Anoud Saud Alshammari and Mohammed A. Amin: Formal analysis, Writing—review and editing. Jing Luo: Writing—review and editing, Supervision, Methodology. Hua Qiu, Jinxuan Jiang, and Yazeed M. Asiri: Writing—review and editing. Runzhou Huang and Hua Hou: Supervision, Methodology, Resources, Project administration. Zeinhom M. El-Bahy and Zhanhu Guo: Writing—review and editing, Writing—original draft, Validation, Resource. Chong Jia, Kaimeng Xu, and Xiangmeng Chen: Writing—review and editing, Supervision, Methodology, Funding acquisition, Validation, Formal analysis.

Declarations

Conflict of Interest The authors declare no interest conflict. They have no known competing financial interests or personal relationships that could have appeared to influence the work reported in this paper. Prof. Zhanhu Guo an editorial board member for Nano-Micro Letters and was not involved in the editorial review or the decision to publish this article.

Open Access This article is licensed under a Creative Commons Attribution 4.0 International License, which permits use, sharing, adaptation, distribution and reproduction in any medium or format, as long as you give appropriate credit to the original author(s) and the source, provide a link to the Creative Commons licence, and indicate if changes were made. The images or other third party material in this article are included in the article’s Creative Commons licence, unless indicated otherwise in a credit line to the material. If material is not included in the article’s Creative Commons licence and your intended use is not permitted by statutory regulation or exceeds the permitted use, you will need to obtain permission directly from the copyright holder. To view a copy of this licence, visit <http://creativecommons.org/licenses/by/4.0/>.

References

1. D.K. Shetty, J. Bhagawati, S. Shetty, L.R. Rodrigues, A. Kumar et al., Enhancing technology acceptance through user experience evaluation: comparative analysis of banking website versus mobile application. *Eng. Sci.* **19**, 154–166 (2022). <https://doi.org/10.30919/es8e678>
2. K. Thenkumari, K.S. Sankaran, J.M. Mathana, Design and implementation of frequency reconfigurable antenna for Wi-Fi applications. *Eng. Sci.* **23**, 876 (2023). <https://doi.org/10.30919/es8d876>
3. S.K. Singh, T. Sharan, A.K. Singh, Enhancing the axial ratio bandwidth of circularly polarized open ground slot CPW-fed antenna for multiband wireless communications. *Eng. Sci.* **17**, 274–284 (2021). <https://doi.org/10.30919/es8d557>
4. X. Zhang, T. Zhang, J. Lu, X. Fu, F. Reveriano et al., The effect of high performance computer on deep neural network. *Eng. Sci.* **15**, 67–79 (2021). <https://doi.org/10.30919/es8d461>
5. A. Yang, B. Li, Z. Yan, M. Yang, A bi-directional carrier sense collision avoidance neighbor discovery algorithm in directional wireless ad hoc sensor networks. *Sensors* **19**, 2120 (2019)
6. T. Li, H. Wei, Y. Zhang, T. Wan, D. Cui et al., Sodium alginate reinforced polyacrylamide/xanthan gum double network ionic hydrogels for stress sensing and self-powered wearable device applications. *Carbohydr. Polym.* **309**, 120678 (2023). <https://doi.org/10.1016/j.carbpol.2023.120678>
7. J. Tang, S. Wu, N. AlMasoud, T.S. Alomar, P. Wasnik et al., Defect passivation in perovskite films by p-methoxy phenylacetonitrile for improved device efficiency and stability. *Adv. Compos. Hybrid Mater.* **6**, 155 (2023). <https://doi.org/10.1007/s42114-023-00732-2>
8. J. Tang, Z. Chen, Y. Ma, H. Zhang, Characterization of wicking performance for open rectangular microgrooves under planar EHD effects in two-phase heat transfer devices. *Eng. Sci.* **19**, 100–113 (2022). <https://doi.org/10.30919/es8d642>
9. G.J. Navathe, S.R. Prasad, A.M. Mane, S.H. Barge, T.D. Donagale et al., A critical review on design and development of new generation energy storage devices. *ES Energy Environ.* **17**, 11–32 (2022). <https://doi.org/10.30919/esee8c739>
10. S. Balsure, V. More, S. Kadam, R. Kadam, A. Kadam et al., Synthesis, structural, magnetic, dielectric and optical properties of co doped Cr-Zn oxide nanoparticles for spintronic devices. *Eng. Sci.* **21**, 774 (2022). <https://doi.org/10.30919/es8d774>
11. G. Wu, X. Gao, K. Wan, Mobility control of unmanned aerial vehicle as communication relay to optimize ground-to-air uplinks. *Sensors* **20**, 2332 (2020)
12. Y. Lu, Y. Yue, Q. Ding, C. Mei, X. Xu et al., Environment-tolerant ionic hydrogel–elastomer hybrids with robust interfaces, high transparency, and biocompatibility for a mechanical–thermal multimode sensor. *InfoMat* **5**, e12409 (2023). <https://doi.org/10.1002/inf2.12409>
13. Z. Li, D. Pan, Z. Han, D.J.P. Kumar, J. Ren et al., Boron nitride whiskers and nano alumina synergistically enhancing the vertical thermal conductivity of epoxy-cellulose aerogel nanocomposites. *Adv. Compos. Hybrid Mater.* **6**, 224 (2023). <https://doi.org/10.1007/s42114-023-00804-3>
14. X. Wang, Z. Liu, H. Wang, C. Zeng et al., Direct 3D printing of piezoelectrets: process feasibility, prototypes fabrication and device performance. *Eng. Sci.* **21**, 800 (2022). <https://doi.org/10.30919/es8d800>

15. Z. Wu, X. Deng, X. Yu, J. Gu, Z.M. El-Bahy et al., Electrospun thermoplastic polyurethane membrane decorated with carbon nanotubes: a platform of flexible strain sensors for human motion monitoring. *Polymer* **303**, 127120 (2024). <https://doi.org/10.1016/j.polymer.2024.127120>
16. C. Wei, M. He, M. Li, X. Ma, W. Dang et al., Hollow Co/NC@MnO₂ polyhedrons with enhanced synergistic effect for high-efficiency microwave absorption. *Mater. Today Phys.* **36**, 101142 (2023). <https://doi.org/10.1016/j.mtphys.2023.101142>
17. D. Jiang, V. Murugadoss, Y. Wang, J. Lin, T. Ding et al., Electromagnetic interference shielding polymers and nanocomposites—A review. *Polym. Rev.* **59**, 280–337 (2019). <https://doi.org/10.1080/15583724.2018.1546737>
18. S. Said, O.E. melhaoui, Y. Guetbach, B. Elhadi, A. Faize, Design of a patch antenna for high-gain applications using one-dimensional electromagnetic band gap structures. *Eng. Sci.* **27**, 1040 (2024). <https://doi.org/10.30919/es1040>
19. L. Wang, J. Cheng, Y. Zou, W. Zheng, Y. Wang et al., Current advances and future perspectives of MXene-based electromagnetic interference shielding materials. *Adv. Compos. Hybrid Mater.* **6**, 172 (2023). <https://doi.org/10.1007/s42114-023-00752-y>
20. S. Zheng, N. Wu, Y. Liu, Q. Wu, Y. Yang et al., Multifunctional flexible, crosslinked composites composed of trashed MXene sediment with high electromagnetic interference shielding performance. *Adv. Compos. Hybrid Mater.* **6**, 161 (2023). <https://doi.org/10.1007/s42114-023-00741-1>
21. J. Liu, M. Wei, H. Li, X. Wang, X. Wang et al., Measurement and mapping of the electromagnetic radiation in the urban environment. *Electromagn. Biol. Med.* **39**, 38–43 (2020). <https://doi.org/10.1080/15368378.2019.1685540>
22. R. Bera, A. Maitra, S. Paria, S.K. Karan, A.K. Das et al., An approach to widen the electromagnetic shielding efficiency in PDMS/ferrous ferric oxide decorated RGO–SWCNH composite through pressure induced tunability. *Chem. Eng. J.* **335**, 501–509 (2018). <https://doi.org/10.1016/j.cej.2017.10.178>
23. X. Zhong, M. He, C. Zhang, Y. Guo, J. Hu et al., Heterostructured BN@Co-C@C endowing polyester composites excellent thermal conductivity and microwave absorption at C band. *Adv. Funct. Mater.* **34**, 2313544 (2024). <https://doi.org/10.1002/adfm.202313544>
24. J. Xiao, B. Zhan, M. He, X. Qi, X. Gong et al., Interfacial polarization loss improvement induced by the hollow engineering of necklace-like PAN/carbon nanofibers for boosted microwave absorption. *Adv. Funct. Mater.* (2024). <https://doi.org/10.1002/adfm.202316722>
25. C. Wei, L. Shi, M. Li, M. He, M. Li et al., Hollow engineering of sandwich NC@Co/NC@MnO₂ composites toward strong wideband electromagnetic wave attenuation. *J. Mater. Sci. Technol.* **175**, 194–203 (2024). <https://doi.org/10.1016/j.jmst.2023.08.020>
26. T. Ma, Y. Zhang, K. Ruan, H. Guo, M. He et al., Advances in 3D printing for polymer composites: a review. *InfoMat* **6**, e12568 (2024). <https://doi.org/10.1002/inf2.12568>
27. M. He, J. Hu, H. Yan, X. Zhong, Y. Zhang et al., Shape anisotropic chain-like CoNi/polydimethylsiloxane composite films with excellent low-frequency microwave absorption and high thermal conductivity. *Adv. Funct. Mater.* (2024). <https://doi.org/10.1002/adfm.202316691>
28. Y. Yi, C. Zhao, H.L. Shindume, J. Ren, L. Chen et al., Enhanced electromagnetic wave absorption of magnetite-spinach derived carbon composite. *Colloids Surf. A Physicochem. Eng. Aspects* **694**, 134149 (2024). <https://doi.org/10.1016/j.colsurfa.2024.134149>
29. F. Li, N. Wu, H. Kimura, Y. Wang, B.B. Xu et al., Initiating binary metal oxides microcubes electrosomagnetic wave absorber toward ultrabroad absorption bandwidth through interfacial and defects modulation. *Nano-Micro Lett.* **15**, 220 (2023). <https://doi.org/10.1007/s40820-023-01197-0>
30. S. Zhang, Z. Jia, B. Cheng, Z. Zhao, F. Lu et al., Recent progress of perovskite oxides and their hybrids for electromagnetic wave absorption: a mini-review. *Adv. Compos. Hybrid Mater.* **5**, 2440–2460 (2022). <https://doi.org/10.1007/s42114-022-00458-7>
31. K. Liu, W. Liu, W. Li, Y. Duan, K. Zhou et al., Strong and highly conductive cellulose nanofibril/silver nanowires nanopaper for high performance electromagnetic interference shielding. *Adv. Compos. Hybrid Mater.* **5**, 1078–1089 (2022). <https://doi.org/10.1007/s42114-022-00425-2>
32. Q. Zhang, D. Lan, S. Deng, J. Gu, Y. Wang et al., Constructing multiple heterogeneous interfaces in one-dimensional carbon fiber materials for superior electromagnetic wave absorption. *Carbon* **226**, 119233 (2024). <https://doi.org/10.1016/j.carbon.2024.119233>
33. N. Wu, B. Zhao, Y. Lian, S. Liu, Y. Xian et al., Metal organic frameworks derived Ni_xSe_y@NC hollow microspheres with modifiable composition and broadband microwave attenuation. *Carbon* **226**, 119215 (2024). <https://doi.org/10.1016/j.carbon.2024.119215>
34. Y. Shi, B. Liang, H. Gao, R. Zhao, Q. Dong et al., Research progress on spherical carbon-based electromagnetic wave absorbing composites. *Carbon* **227**, 119244 (2024). <https://doi.org/10.1016/j.carbon.2024.119244>
35. S. Zhang, D. Lan, J. Zheng, J. Kong, J. Gu et al., Perspectives of nitrogen-doped carbons for electromagnetic wave absorption. *Carbon* **221**, 118925 (2024). <https://doi.org/10.1016/j.carbon.2024.118925>
36. J. Yan, Z. Ye, D. Lan, W. Chen, Z. Jia et al., Transition metal carbides towards electromagnetic wave absorption application: state of the art and perspectives. *Compos. Commun.* **48**, 101954 (2024). <https://doi.org/10.1016/j.coco.2024.101954>
37. B. Miao, Y. Cao, Q. Zhu, M.A. Nawaz, J.A. Ordiozola et al., Scalable synthesis of 2D Ti₂CT_x MXene and molybdenum disulfide composites with excellent microwave absorbing performance. *Adv. Compos. Hybrid Mater.* **6**, 61 (2023). <https://doi.org/10.1007/s42114-023-00643-2>
38. H. Cheng, Y. Pan, Q. Chen, R. Che, G. Zheng et al., Ultrathin flexible poly(vinylidene fluoride)/MXene/silver nanowire film with outstanding specific EMI shielding and high heat



- dissipation. *Adv. Compos. Hybrid Mater.* **4**, 505–513 (2021). <https://doi.org/10.1007/s42114-021-00224-1>
39. N. Wu, B. Zhao, X. Chen, C. Hou, M. Huang et al., Dielectric properties and electromagnetic simulation of molybdenum disulfide and ferric oxide-modified $\text{Ti}_3\text{C}_2\text{T}_x$ MXene heterostructure for potential microwave absorption. *Adv. Compos. Hybrid Mater.* **5**, 1548–1556 (2022). <https://doi.org/10.1007/s42114-022-00490-7>
40. Y. Wang, P. Wang, Z. Du, C. Liu, C. Shen et al., Electromagnetic interference shielding enhancement of poly(lactic acid)-based carbonaceous nanocomposites by poly(ethylene oxide)-assisted segregated structure: a comparative study of carbon nanotubes and graphene nanoplatelets. *Adv. Compos. Hybrid Mater.* **5**, 209–219 (2022). <https://doi.org/10.1007/s42114-021-00320-2>
41. B. Wen, M. Cao, M. Lu, W. Cao, H. Shi et al., Reduced graphene oxides: light-weight and high-efficiency electromagnetic interference shielding at elevated temperatures. *Adv. Mater.* **26**, 3484–3489 (2014). <https://doi.org/10.1002/adma.201400108>
42. D. Lan, Y. Wang, Y. Wang, X. Zhu, H. Li et al., Impact mechanisms of aggregation state regulation strategies on the microwave absorption properties of flexible polyaniline. *J. Colloid Interface Sci.* **651**, 494–503 (2023). <https://doi.org/10.1016/j.jcis.2023.08.019>
43. J. Guo, Z. Chen, X. Xu, X. Li, H. Liu et al., Enhanced electromagnetic wave absorption of engineered epoxy nanocomposites with the assistance of polyaniline fillers. *Adv. Compos. Hybrid Mater.* **5**, 1769–1777 (2022). <https://doi.org/10.1007/s42114-022-00417-2>
44. Y.-J. Wan, P.-L. Zhu, S.-H. Yu, R. Sun, C.-P. Wong et al., Anticorrosive, ultralight, and flexible carbon-wrapped metallic nanowire hybrid sponges for highly efficient electromagnetic interference shielding. *Small* **14**, e1800534 (2018). <https://doi.org/10.1002/sml.201800534>
45. M. Arjmand, A.A. Moud, Y. Li, U. Sundararaj, Outstanding electromagnetic interference shielding of silver nanowires: comparison with carbon nanotubes. *RSC Adv.* **5**, 56590–56598 (2015). <https://doi.org/10.1039/C5RA08118A>
46. T. Gao, Y. Ma, L. Ji, Y. Zheng, S. Yan et al., Nickel-coated wood-derived porous carbon (Ni/WPC) for efficient electromagnetic interference shielding. *Adv. Compos. Hybrid Mater.* **5**, 2328–2338 (2022). <https://doi.org/10.1007/s42114-022-00420-7>
47. Z. Cui, J. Zhou, X. Wang, Q. Wang, J. Si et al., *In situ* growth of bimetallic nickel cobalt sulfide (NiCo_2S_4) nanowire arrays encapsulated by nitrogen-doped carbon on carbon cloth as binder-free and flexible electrode for high-performance aqueous Zn batteries. *Adv. Compos. Hybrid Mater.* **6**, 95 (2023). <https://doi.org/10.1007/s42114-023-00668-7>
48. Z. Zhou, D. Lan, J. Ren, Y. Cheng, Z. Jia et al., Controllable heterogeneous interfaces and dielectric modulation of biomass-derived nanosheet metal-sulfide complexes for high-performance electromagnetic wave absorption. *J. Mater. Sci. Technol.* **185**, 165–173 (2024). <https://doi.org/10.1016/j.jmst.2023.11.010>
49. J. Yin, W. Ma, Z. Gao, X. Lei, C. Jia, A review of electromagnetic shielding fabric, wave-absorbing fabric and wave-transparent fabric. *Polymers* **14**, 377 (2022). <https://doi.org/10.3390/polym14030377>
50. J. Chang, H. Zhai, Z. Hu, J. Li, Ultra-thin metal composites for electromagnetic interference shielding. *Compos. Part B Eng.* **246**, 110269 (2022). <https://doi.org/10.1016/j.compositesb.2022.110269>
51. Q. Zhang, Q. Liang, Z. Zhang, Z. Kang, Q. Liao et al., Electromagnetic shielding hybrid nanogenerator for health monitoring and protection. *Adv. Funct. Mater.* **28**, 1703801 (2018). <https://doi.org/10.1002/adfm.201703801>
52. N. Wu, X. Liu, C. Zhao, C. Cui, A. Xia, Effects of particle size on the magnetic and microwave absorption properties of carbon-coated nickel nanocapsules. *J. Alloys Compd.* **656**, 628–634 (2016). <https://doi.org/10.1016/j.jallcom.2015.10.027>
53. X.F. Zhang, X.L. Dong, H. Huang, Y.Y. Liu, W.N. Wang et al., Microwave absorption properties of the carbon-coated nickel nanocapsules. *Appl. Phys. Lett.* **89**, 053115 (2006). <https://doi.org/10.1063/1.2236965>
54. H. Wang, H. Zhang, K. Zhao, A. Nie, S. Alharthi et al., Research progress on electromagnetic wave absorption based on magnetic metal oxides and their composites. *Adv. Compos. Hybrid Mater.* **6**, 120 (2023). <https://doi.org/10.1007/s42114-023-00694-5>
55. J. Bednárek, L. Matějová, Z. Jankovská, M. Vaštyl, B. Sokolová et al., The influence of structural properties on the adsorption capacities of microwave-assisted biochars for metazachlor removal from aqueous solutions. *J. Environ. Chem. Eng.* **10**, 108003 (2022). <https://doi.org/10.1016/j.jece.2022.108003>
56. L. Zhang, B.-W. Liu, Y.-Z. Wang, T. Fu, H.-B. Zhao, P-doped PANI/AgMWs nano/micro coating towards high-efficiency flame retardancy and electromagnetic interference shielding. *Compos. Part B Eng.* **238**, 109944 (2022). <https://doi.org/10.1016/j.compositesb.2022.109944>
57. L. Zou, C. Lan, S. Zhang, X. Zheng, Z. Xu et al., Near-instantaneously self-healing coating toward stable and durable electromagnetic interference shielding. *Nano-Micro Lett.* **13**, 190 (2021). <https://doi.org/10.1007/s40820-021-00709-0>
58. Y. Li, X. Chen, Q. Wei, W. Liu, Y. Zhang et al., Oxygen-sulfur Co-substitutional Fe@C nanocapsules for improving microwave absorption properties. *Sci. Bull.* **65**, 623–630 (2020). <https://doi.org/10.1016/j.scib.2020.01.009>
59. R. Sun, H.-B. Zhang, J. Liu, X. Xie, R. Yang et al., Highly conductive transition metal carbide/carbonitride(MXene)@ polystyrene nanocomposites fabricated by electrostatic assembly for highly efficient electromagnetic interference shielding. *Adv. Funct. Mater.* **27**, 1702807 (2017). <https://doi.org/10.1002/adfm.201702807>
60. J. Xu, R. Li, S. Ji, B. Zhao, T. Cui et al., Multifunctional graphene microstructures inspired by honeycomb for ultra-high performance electromagnetic interference shielding and wearable applications. *ACS Nano* **15**, 8907–8918 (2021). <https://doi.org/10.1021/acsnano.1c01552>

61. L. Wang, H. Qiu, P. Song, Y. Zhang, Y. Lu et al., 3D $\text{Ti}_3\text{C}_2\text{T}_x$ MXene/C hybrid foam/epoxy nanocomposites with superior electromagnetic interference shielding performances and robust mechanical properties. *Compos. Part A Appl. Sci. Manuf.* **123**, 293–300 (2019). <https://doi.org/10.1016/j.compositesa.2019.05.030>
62. Z. Wang, R. Wei, J. Gu, H. Liu, C. Liu et al., Ultralight, highly compressible and fire-retardant graphene aerogel with self-adjustable electromagnetic wave absorption. *Carbon* **139**, 1126–1135 (2018). <https://doi.org/10.1016/j.carbon.2018.08.014>
63. Y. Jiao, C. Wan, W. Zhang, W. Bao, J. Li, Carbon fibers encapsulated with nano-copper: a core-shell structured composite for antibacterial and electromagnetic interference shielding applications. *Nanomaterials (Basel)* **9**, 460 (2019). <https://doi.org/10.3390/nano9030460>
64. C. Wan, J. Li, Synthesis and electromagnetic interference shielding of cellulose-derived carbon aerogels functionalized with $\alpha\text{-Fe}_2\text{O}_3$ and polypyrrole. *Carbohydr. Polym.* **161**, 158–165 (2017). <https://doi.org/10.1016/j.carbpol.2017.01.003>
65. C. Wan, Y. Jiao, T. Qiang, J. Li, Cellulose-derived carbon aerogels supported goethite ($\alpha\text{-FeOOH}$) nanoneedles and nanoflowers for electromagnetic interference shielding. *Carbohydr. Polym.* **156**, 427–434 (2017). <https://doi.org/10.1016/j.carbpol.2016.09.028>
66. X.Y. Jiang, Q.K. Zhang, S.P. Deng, B. Zhou, B. Wang et al., Enhanced thermoelectric performance of polythiophene/carbon nanotube-based composites. *J. Electron. Mater.* **49**, 2371–2380 (2020). <https://doi.org/10.1007/s11664-019-07935-8>
67. Y. Long, Z. Zhang, K. Sun, C. Wang, N. Zeng et al., Enhanced electromagnetic wave absorption performance of hematite@carbon nanotubes/polyacrylamide hydrogel composites with good flexibility and biocompatibility. *Adv. Compos. Hybrid Mater.* **6**, 173 (2023). <https://doi.org/10.1007/s42114-023-00749-7>
68. Y. Huang, G. Liu, D. Liu, M. Hao, P. Xie et al., Excellent microwave absorption performance in porous Co/C nanocomposites by biomass conversion. *ES Food Agrofor.* **12**, 888 (2023). <https://doi.org/10.30919/esfaf888>
69. S.H. Kim, W.I. Choi, K.H. Kim, D.J. Yang, S. Heo et al., Nanoscale chemical and electrical stabilities of graphene-covered silver nanowire networks for transparent conducting electrodes. *Sci. Rep.* **6**, 33074 (2016). <https://doi.org/10.1038/srep33074>
70. N. Ucar, B.K. Kayaoğlu, A. Bilge, G. Gurel, P. Sencandan et al., Electromagnetic shielding effectiveness of carbon fabric/epoxy composite with continuous graphene oxide fiber and multiwalled carbon nanotube. *J. Compos. Mater.* **52**, 3341–3350 (2018). <https://doi.org/10.1177/0021998318765273>
71. Y. Zhong, D. Liu, Q. Yang, Y. Qu, C. Yu et al., Boosting microwave absorption performance of bio-gel derived Co/C nanocomposites. *Eng. Sci.* **26**, 988 (2023). <https://doi.org/10.30919/es988>
72. S.-S. Wang, D.-Y. Feng, Z.-M. Zhang, X. Liu, K.-P. Ruan et al., Highly thermally conductive polydimethylsiloxane composites with controllable 3D GO@f-CNTs networks via self-sacrificing template method. *Chin. J. Polym. Sci.* **42**, 897–906 (2024). <https://doi.org/10.1007/s10118-024-3098-4>
73. C. Tang, S. Zhang, J. Zhang, X. Zhang, Z. Hang et al., Silicon carbide coated carbon nanotube porous sponge with super elasticity, low density, high thermal resistivity, and synergistically enhanced electromagnetic interference shielding performances. *Chem. Eng. J.* **469**, 144011 (2023). <https://doi.org/10.1016/j.ccej.2023.144011>
74. H. Abbasi, M. Antunes, J.I. Velasco, Recent advances in carbon-based polymer nanocomposites for electromagnetic interference shielding. *Prog. Mater. Sci.* **103**, 319–373 (2019). <https://doi.org/10.1016/j.pmatsci.2019.02.003>
75. H. Wang, J. Fu, C. Wang, J. Wang, A. Yang et al., A binder-free high silicon content flexible anode for Li-ion batteries. *Energy Environ. Sci.* **13**, 848–858 (2020). <https://doi.org/10.1039/c9ee02615k>
76. C. Wang, H. Wang, B. Dang, Z. Wang, X. Shen et al., Ultra-high yield of nitrogen doped porous carbon from biomass waste for supercapacitor. *Renew. Energy* **156**, 370–376 (2020). <https://doi.org/10.1016/j.renene.2020.04.092>
77. Y. Chen, J. Fu, B. Dang, Q. Sun, H. Li et al., Artificial wooden nacre: a high specific strength engineering material. *ACS Nano* **14**, 2036–2043 (2020). <https://doi.org/10.1021/acsnano.9b08647>
78. G. Chen, T. Li, C. Chen, C. Wang, Y. Liu et al., A highly conductive cationic wood membrane. *Adv. Funct. Mater.* **29**, 1902772 (2019). <https://doi.org/10.1002/adfm.201902772>
79. X. Han, Y. Ye, F. Lam, J. Pu, F. Jiang, Hydrogen-bonding-induced assembly of aligned cellulose nanofibers into ultratrong and tough bulk materials. *J. Mater. Chem. A* **7**, 27023–27031 (2019). <https://doi.org/10.1039/C9TA11118B>
80. A.N. Subba Rao, G.B. Nagarajappa, S. Nair, A.M. Chathoth, K.K. Pandey, Flexible transparent wood prepared from poplar veneer and polyvinyl alcohol. *Compos. Sci. Technol.* **182**, 107719 (2019). <https://doi.org/10.1016/j.compscitech.2019.107719>
81. W. Cao, W. Zhang, L. Dong, Z. Ma, J. Xu et al., Progress on quantum dot photocatalysts for biomass valorization. *Exploration* **3**, 20220169 (2023). <https://doi.org/10.1002/exp.20220169>
82. Y. Xing, Y. Xue, J. Song, Y. Sun, L. Huang et al., Superhydrophobic coatings on wood substrate for self-cleaning and EMI shielding. *Appl. Surf. Sci.* **436**, 865–872 (2018). <https://doi.org/10.1016/j.apsusc.2017.12.083>
83. W. He, J. Li, J. Tian, H. Jing, Y. Li, Characteristics and properties of wood/polyaniline electromagnetic shielding composites synthesized via *in situ* polymerization. *Polym. Compos.* **39**, 537–543 (2018). <https://doi.org/10.1002/pc.23966>
84. W. Gan, C. Chen, M. Giroux, G. Zhong, M.M. Goyal et al., Conductive wood for high-performance structural electromagnetic interference shielding. *Chem. Mater.* **32**, 5280–5289 (2020). <https://doi.org/10.1021/acs.chemmater.0c01507>

85. L. Xiang, A.K. Darboe, Z. Luo, X. Qi, J.-J. Shao et al., Constructing two-dimensional/two-dimensional reduced graphene oxide/MoX₂ (X = Se and S) van der Waals heterojunctions: a combined composition modulation and interface engineering strategy for microwave absorption. *Adv. Compos. Hybrid Mater.* **6**, 215 (2023). <https://doi.org/10.1007/s42114-023-00793-3>
86. Q. Guo, Y. Pan, D. Yin, Y. Wang, J. Huang, High hydrophobic wood/Cu-Fe₃O₄@graphene/Ni composites for electromagnetic interference shielding. *J. Inorg. Organomet. Polym. Mater.* **33**, 502–514 (2023). <https://doi.org/10.1007/s10904-022-02512-9>
87. Y. Hui, W. Xie, H. Gu, Reduced graphene oxide/nanocellulose/amino-multiwalled carbon nanotubes nanocomposite aerogel for excellent oil adsorption. *ES Food Agrofor.* **5**, 38–44 (2021). <https://doi.org/10.30919/esfaf531>
88. Z. Sun, H. Qi, M. Chen, S. Guo, Z. Huang et al., Progress in cellulose/carbon nanotube composite flexible electrodes for supercapacitors. *Eng. Sci.* **18**, 59–74 (2022). <https://doi.org/10.30919/es8d588>
89. C. Sang, S. Wang, X. Jin, X. Cheng, H. Xiao et al., Nanocellulose-mediated conductive hydrogels with NIR photoreponse and fatigue resistance for multifunctional wearable sensors. *Carbohydr. Polym.* **333**, 121947 (2024). <https://doi.org/10.1016/j.carbpol.2024.121947>
90. D. Pan, G. Yang, H.M. Abo-Dief, J. Dong, F. Su et al., Vertically aligned silicon carbide nanowires/boron nitride cellulose aerogel networks enhanced thermal conductivity and electromagnetic absorbing of epoxy composites. *Nano-Micro Lett.* **14**, 118 (2022). <https://doi.org/10.1007/s40820-022-00863-z>
91. G. Han, Z. Ma, B. Zhou, C. He, B. Wang et al., Cellulose-based Ni-decorated graphene magnetic film for electromagnetic interference shielding. *J. Colloid Interface Sci.* **583**, 571–578 (2021). <https://doi.org/10.1016/j.jcis.2020.09.072>
92. Q. Zhang, L. Ning, C. Wang, M. Wang, Y. Shen et al., Study of an energy-efficient and cost-friendly electromagnetic shielding material with three-dimensional conductive network fabricated by dispersing Ni-Fe-P alloys coated bamboo fibers in a HDPE matrix. *J. Mater. Sci. Mater. Electron.* **30**, 14631–14645 (2019). <https://doi.org/10.1007/s10854-019-01835-7>
93. Y. Gu, D. Wang, Y. Gao, Y. Yue, W. Yang et al., Solar-powered high-performance lignin-wood evaporator for solar steam generation. *Adv. Funct. Mater.* **33**, 2306947 (2023). <https://doi.org/10.1002/adfm.202306947>
94. C. Wu, L. Zeng, G. Chang, Y. Zhou, K. Yan et al., Composite phase change materials embedded into cellulose/polyacrylamide/graphene nanosheets/silver nanowire hybrid aerogels simultaneously with effective thermal management and anisotropic electromagnetic interference shielding. *Adv. Compos. Hybrid Mater.* **6**, 31 (2023). <https://doi.org/10.1007/s42114-022-00618-9>
95. W. Wang, Y. Liu, S. Li, K. Dong, S. Wang et al., Lead-free and wearing comfort 3D composite fiber-needed fabric for highly efficient X-ray shielding. *Adv. Compos. Hybrid Mater.* **6**, 76 (2023). <https://doi.org/10.1007/s42114-023-00642-3>
96. J.-W. Gu, D.-J. Wang, Special issue: functional polymer materials. *Chin. J. Polym. Sci.* **42**, 895–896 (2024). <https://doi.org/10.1007/s10118-024-3165-x>
97. W. Yuan, J. Yang, F. Yin, Y. Li, Y. Yuan, Flexible and stretchable MXene/Polyurethane fabrics with delicate wrinkle structure design for effective electromagnetic interference shielding at a dynamic stretching process. *Compos. Commun.* **19**, 90–98 (2020). <https://doi.org/10.1016/j.coco.2020.03.003>
98. W. Cao, C. Ma, S. Tan, M. Ma, P. Wan et al., Ultrathin and flexible CNTs/MXene/cellulose nanofibrils composite paper for electromagnetic interference shielding. *Nano-Micro Lett.* **11**, 72 (2019). <https://doi.org/10.1007/s40820-019-0304-y>
99. T. Zhao, J. Zhou, W. Wu, K. Qian, Y. Zhu et al., Antibacterial conductive polyacrylamide/quaternary ammonium chitosan hydrogel for electromagnetic interference shielding and strain sensing. *Int. J. Biol. Macromol.* **265**, 130795 (2024). <https://doi.org/10.1016/j.ijbiomac.2024.130795>
100. W. Yang, Z. Zhao, K. Wu, R. Huang, T. Liu et al., Ultrathin flexible reduced graphene oxide/cellulose nanofiber composite films with strongly anisotropic thermal conductivity and efficient electromagnetic interference shielding. *J. Mater. Chem. C* **5**, 3748–3756 (2017). <https://doi.org/10.1039/C7TC00400A>
101. Z.-H. Zhou, Y. Liang, H.-D. Huang, L. Li, B. Yang et al., Structuring dense three-dimensional sheet-like skeleton networks in biomass-derived carbon aerogels for efficient electromagnetic interference shielding. *Carbon* **152**, 316–324 (2019). <https://doi.org/10.1016/j.carbon.2019.06.027>
102. X. Ma, B. Shen, L. Zhang, Z. Chen, Y. Liu et al., Novel straw-derived carbon materials for electromagnetic interference shielding: a waste-to-wealth and sustainable initiative. *ACS Sustainable Chem. Eng.* **7**, 9663–9670 (2019). <https://doi.org/10.1021/acssuschemeng.9b01288>
103. S. Li, J. Li, N. Ma, D. Liu, G. Sui, Super-compression-resistant multiwalled carbon nanotube/nickel-coated carbonized loofah fiber/polyether ether ketone composite with excellent electromagnetic shielding performance. *ACS Sustainable Chem. Eng.* **7**, 13970–13980 (2019). <https://doi.org/10.1021/acssuschemeng.9b02447>
104. X.-Y. Ye, Y. Chen, J. Yang, H.-Y. Yang, D.-W. Wang et al., Sustainable wearable infrared shielding bamboo fiber fabrics loaded with antimony doped tin oxide/silver binary nanoparticles. *Adv. Compos. Hybrid Mater.* **6**, 106 (2023). <https://doi.org/10.1007/s42114-023-00683-8>
105. X. Wan, Y. Zhao, Z. Li, L. Li, Emerging polymeric electrospun fibers: From structural diversity to application in flexible bioelectronics and tissue engineering. *Exploration (Beijing)* **2**, 20210029 (2022). <https://doi.org/10.1002/EXP.20210029>
106. Q. Wang, Z. Liang, F. Li, J. Lee, L.E. Low et al., Dynamically switchable magnetic resonance imaging contrast agents. *Exploration (Beijing)* **1**, 20210009 (2021). <https://doi.org/10.1002/EXP.20210009>
107. J. Cheng, C. Li, Y. Xiong, H. Zhang, H. Raza et al., Recent advances in design strategies and multifunctionality of

- flexible electromagnetic interference shielding materials. *Nano-Micro Lett.* **14**, 80 (2022). <https://doi.org/10.1007/s40820-022-00823-7>
108. L. Yang, R. Jie, H.-T. Jiang, S. Yong, C. Hong, Quantum spin Hall effect in metamaterials. *Acta Phys. Sin.* **66**, 227803 (2017). <https://doi.org/10.7498/aps.66.227803>
109. E. Hosseini, M. Arjmand, U. Sundararaj, K. Karan, Filler-free conducting polymers as a new class of transparent electromagnetic interference shields. *ACS Appl. Mater. Interfaces* **12**, 28596–28606 (2020). <https://doi.org/10.1021/acsami.0c03544>
110. Y. Liu, Z. Jia, Q. Zhan, Y. Dong, Q. Xu et al., Magnetic manganese-based composites with multiple loss mechanisms towards broadband absorption. *Nano Res.* **15**, 5590–5600 (2022). <https://doi.org/10.1007/s12274-022-4287-5>
111. P. Song, B. Liu, H. Qiu, X. Shi, D. Cao et al., MXenes for polymer matrix electromagnetic interference shielding composites: a review. *Compos. Commun.* **24**, 100653 (2021). <https://doi.org/10.1016/j.coco.2021.100653>
112. S.H. Lee, S. Yu, F. Shahzad, W.N. Kim, C. Park et al., Density-tunable lightweight polymer composites with dual-functional ability of efficient EMI shielding and heat dissipation. *Nanoscale* **9**, 13432–13440 (2017). <https://doi.org/10.1039/C7NR02618H>
113. H. Guo, Y. Chen, Y. Li, W. Zhou, W. Xu et al., Electrospun fibrous materials and their applications for electromagnetic interference shielding: a review. *Compos. Part A Appl. Sci. Manuf.* **143**, 106309 (2021). <https://doi.org/10.1016/j.compositesa.2021.106309>
114. C. Liang, Z. Gu, Y. Zhang, Z. Ma, H. Qiu et al., Structural design strategies of polymer matrix composites for electromagnetic interference shielding: a review. *Nano-Micro Lett.* **13**, 181 (2021). <https://doi.org/10.1007/s40820-021-00707-2>
115. R. Ravindren, S. Mondal, K. Nath, N.C. Das, Investigation of electrical conductivity and electromagnetic interference shielding effectiveness of preferentially distributed conductive filler in highly flexible polymer blends nanocomposites. *Compos. Part A Appl. Sci. Manuf.* **118**, 75–89 (2019). <https://doi.org/10.1016/j.compositesa.2018.12.012>
116. V. Shukla, Review of electromagnetic interference shielding materials fabricated by iron ingredients. *Nanoscale Adv.* **1**, 1640–1671 (2019). <https://doi.org/10.1039/C9NA00108E>
117. Y. Cheng, W. Zhu, X. Lu, C. Wang, Recent progress of electrospun nanofibrous materials for electromagnetic interference shielding. *Compos. Commun.* **27**, 100823 (2021). <https://doi.org/10.1016/j.coco.2021.100823>
118. Y. Huangfu, C. Liang, Y. Han, H. Qiu, P. Song et al., Fabrication and investigation on the Fe_3O_4 /thermally annealed graphene aerogel/epoxy electromagnetic interference shielding nanocomposites. *Compos. Sci. Technol.* **169**, 70–75 (2019). <https://doi.org/10.1016/j.compscitech.2018.11.012>
119. C. Xiong, T. Wang, Y. Zhang, M. Zhu, Y. Ni, Recent progress on green electromagnetic shielding materials based on macro wood and micro cellulose components from natural agricultural and forestry resources. *Nano Res.* **15**, 7506–7532 (2022). <https://doi.org/10.1007/s12274-022-4512-2>
120. R. Liu, M. Miao, Y. Li, J. Zhang, S. Cao et al., Ultrathin biomimetic polymeric $\text{Ti}_3\text{C}_2\text{T}_x$ MXene composite films for electromagnetic interference shielding. *ACS Appl. Mater. Interfaces* **10**, 44787–44795 (2018). <https://doi.org/10.1021/acsami.8b18347>
121. Z. Zeng, F. Jiang, Y. Yue, D. Han, L. Lin et al., Flexible and ultrathin waterproof cellular membranes based on high-conjunction metal-wrapped polymer nanofibers for electromagnetic interference shielding. *Adv. Mater.* **32**, e1908496 (2020). <https://doi.org/10.1002/adma.201908496>
122. H.C. Chen, K.C. Lee, J.H. Lin, A. Koch, Fabrication of conductive woven fabric and analysis of electromagnetic shielding via measurement and empirical Eq. *J Mater Process Tech.* **184**, 124–130 (2007). <https://doi.org/10.1016/j.jmatprotec.2006.11.030>
123. S.A. Hashemi, A. Ghaffarkhah, E. Hosseini, S. Bahrani, P. Najmi et al., Recent progress on hybrid fibrous electromagnetic shields: Key protectors of living species against electromagnetic radiation. *Matter* **5**, 3807–3868 (2022). <https://doi.org/10.1016/j.matt.2022.09.012>
124. L. Wang, P. Song, C.-T. Lin, J. Kong, J. Gu, 3D shapeable, superior electrically conductive cellulose nanofibers/ $\text{Ti}_3\text{C}_2\text{T}_x$ MXene aerogels/epoxy nanocomposites for promising EMI shielding. *Research* **2020**, 4093732 (2020). <https://doi.org/10.34133/2020/4093732>
125. M. Cheng, M. Ying, R. Zhao, L. Ji, H. Li et al., Transparent and flexible electromagnetic interference shielding materials by constructing sandwich AgNW@MXene/wood composites. *ACS Nano* **16**, 16996–17007 (2022). <https://doi.org/10.1021/acsnano.2c07111>
126. Z. Zeng, C. Wang, Y. Zhang, P. Wang, S.I. Seyed Shahabadi et al., Ultralight and highly elastic graphene/lignin-derived carbon nanocomposite aerogels with ultrahigh electromagnetic interference shielding performance. *ACS Appl. Mater. Interfaces* **10**, 8205–8213 (2018). <https://doi.org/10.1021/acsami.7b19427>
127. F. Luo, D. Liu, T. Cao, H. Cheng, J. Kuang et al., Study on broadband microwave absorbing performance of gradient porous structure. *Adv. Compos. Hybrid Mater.* **4**, 591–601 (2021). <https://doi.org/10.1007/s42114-021-00275-4>
128. Y. Zhang, S.-H. Yang, Y. Xin, B. Cai, P.-F. Hu et al., Designing symmetric gradient honeycomb structures with carbon-coated iron-based composites for high-efficiency microwave absorption. *Nano-Micro Lett.* **16**, 234 (2024). <https://doi.org/10.1007/s40820-024-01435-z>
129. Y. Wang, W. Zhao, L. Tan, Y. Li, L. Qin et al., Review of polymer-based composites for electromagnetic shielding application. *Molecules* **28**, 5628 (2023). <https://doi.org/10.3390/molecules28155628>
130. Z. Dai, C. Hu, Y. Wei, W. Zhang, J. Xu et al., Highly anisotropic carbonized wood as electronic materials for electromagnetic interference shielding and thermal management. *Adv. Electron. Mater.* **9**, 2300162 (2023). <https://doi.org/10.1002/aelm.202300162>
131. T. Chu, Y. Gao, L. Yi, C. Fan, L. Yan et al., Highly fire-retardant optical wood enabled by transparent fireproof coatings.

- Adv. Compos. Hybrid Mater. **5**, 1821–1829 (2022). <https://doi.org/10.1007/s42114-022-00440-3>
132. C. Chen, Y. Kuang, S. Zhu, I. Burgert, T. Keplinger et al., Structure–property–function relationships of natural and engineered wood. *Nat. Rev. Mater.* **5**, 642–666 (2020). <https://doi.org/10.1038/s41578-020-0195-z>
133. M. Saiful Islam, S. Hamdan, I. Jusoh, M. Rezaur Rahman, A.S. Ahmed, The effect of alkali pretreatment on mechanical and morphological properties of tropical wood polymer composites. *Mater. Des.* **33**, 419–424 (2012). <https://doi.org/10.1016/j.matdes.2011.04.044>
134. S. Ge, H. Ouyang, H. Ye, Y. Shi, Y. Sheng et al., High-performance and environmentally friendly acrylonitrile butadiene styrene/wood composite for versatile applications in furniture and construction. *Adv. Compos. Hybrid Mater.* **6**, 44 (2023). <https://doi.org/10.1007/s42114-023-00628-1>
135. Y. Zhang, K. Ruan, K. Zhou, J. Gu, Controlled distributed $Ti_3C_2T_x$ hollow microspheres on thermally conductive polyimide composite films for excellent electromagnetic interference shielding. *Adv. Mater.* **35**, 2211642 (2023). <https://doi.org/10.1002/adma.202211642>
136. Y. Guo, K. Ruan, G. Wang, J. Gu, Advances and mechanisms in polymer composites toward thermal conduction and electromagnetic wave absorption. *Sci. Bull.* **68**, 1195–1212 (2023). <https://doi.org/10.1016/j.scib.2023.04.036>
137. C.J. Zhang, B. Anasori, A. Seral-Ascaso, S.H. Park, N. McEvoy et al., Transparent, flexible, and conductive 2D titanium carbide (MXene) films with high volumetric capacitance. *Adv. Mater.* **29**, 1702678 (2017). <https://doi.org/10.1002/adma.201702678>
138. X. Zeng, X. Jiang, Y. Ning, Y. Gao, R. Che, Constructing built-in electric fields with semiconductor junctions and Schottky junctions based on Mo-MXene/Mo-metal sulfides for electromagnetic response. *Nano-Micro Lett.* **16**, 213 (2024). <https://doi.org/10.1007/s40820-024-01449-7>
139. M.-S. Cao, Y.-Z. Cai, P. He, J.-C. Shu, W.-Q. Cao et al., 2D MXenes: Electromagnetic property for microwave absorption and electromagnetic interference shielding. *Chem. Eng. J.* **359**, 1265–1302 (2019). <https://doi.org/10.1016/j.cej.2018.11.051>
140. J. Halim, K.M. Cook, M. Naguib, P. Eklund, Y. Gogotsi et al., X-ray photoelectron spectroscopy of select multi-layered transition metal carbides (MXenes). *Appl. Surf. Sci.* **362**, 406–417 (2016). <https://doi.org/10.1016/j.apsusc.2015.11.089>
141. J. Zhang, N. Kong, S. Uzun, A. Levitt, S. Seyedin et al., Scalable manufacturing of free-standing, strong $Ti_3C_2T_x$ MXene films with outstanding conductivity. *Adv. Mater.* **32**, e2001093 (2020). <https://doi.org/10.1002/adma.202001093>
142. Y. Wei, C. Hu, Z. Dai, Y. Zhang, W. Zhang et al., Highly anisotropic MXene@Wood composites for tunable electromagnetic interference shielding. *Compos. Part A Appl. Sci. Manuf.* **168**, 107476 (2023). <https://doi.org/10.1016/j.compositesa.2023.107476>
143. Y. Wei, Z. Dai, Y. Zhang, W. Zhang, J. Gu et al., Multifunctional waterproof MXene-coated wood with high electromagnetic shielding performance. *Cellulose* **29**, 5883–5893 (2022). <https://doi.org/10.1007/s10570-022-04609-3>
144. J. Liu, H.-B. Zhang, R. Sun, Y. Liu, Z. Liu et al., Hydrophobic, flexible, and lightweight MXene foams for high-performance electromagnetic-interference shielding. *Adv. Mater.* **29**, 1702367 (2017). <https://doi.org/10.1002/adma.201702367>
145. Y. Jiang, X. Ru, W. Che, Z. Jiang, H. Chen et al., Flexible, mechanically robust and self-extinguishing MXene/wood composite for efficient electromagnetic interference shielding. *Compos. Part B Eng.* **229**, 109460 (2022). <https://doi.org/10.1016/j.compositesb.2021.109460>
146. Z. Wang, X. Han, S. Wang, X. Han, J. Pu, MXene/wood-based composite materials with electromagnetic shielding properties. *Holzforschung* **75**, 494–499 (2021). <https://doi.org/10.1515/hf-2020-0090>
147. Z. Wang, X. Han, X. Han, Z. Chen, S. Wang et al., MXene/wood-derived hierarchical cellulose scaffold composite with superior electromagnetic shielding. *Carbohydr. Polym.* **254**, 117033 (2021). <https://doi.org/10.1016/j.carbpol.2020.117033>
148. Y. Wei, D. Liang, H. Zhou, S. Huang, W. Zhang et al., Facile preparation of MXene-decorated wood with excellent electromagnetic interference shielding performance. *Compos. Part A Appl. Sci. Manuf.* **153**, 106739 (2022). <https://doi.org/10.1016/j.compositesa.2021.106739>
149. C. Liang, H. Qiu, P. Song, X. Shi, J. Kong et al., Ultra-light MXene aerogel/wood-derived porous carbon composites with wall-like “mortar/brick” structures for electromagnetic interference shielding. *Sci. Bull.* **65**, 616–622 (2020). <https://doi.org/10.1016/j.scib.2020.02.009>
150. S. Bai, X. Guo, X. Zhang, X. Zhao, H. Yang, $Ti_3C_2T_x$ MXene-AgNW composite flexible transparent conductive films for EMI shielding. *Compos. Part A Appl. Sci. Manuf.* **149**, 106545 (2021). <https://doi.org/10.1016/j.compositesa.2021.106545>
151. S. Zhu, S. Kumar Biswas, Z. Qiu, Y. Yue, Q. Fu et al., Transparent wood-based functional materials via a top-down approach. *Prog. Mater. Sci.* **132**, 101025 (2023). <https://doi.org/10.1016/j.pmatsci.2022.101025>
152. M. Han, C.E. Shuck, R. Rakhmanov, D. Parchment, B. Anasori et al., Beyond $Ti_3C_2T_x$: MXenes for electromagnetic interference shielding. *ACS Nano* **14**, 5008–5016 (2020). <https://doi.org/10.1021/acsnano.0c01312>
153. A. Iqbal, J. Kwon, M.-K. Kim, C.M. Koo, MXenes for electromagnetic interference shielding: Experimental and theoretical perspectives. *Mater. Today Adv.* **9**, 100124 (2021). <https://doi.org/10.1016/j.mtadv.2020.100124>
154. Z. Wang, K. Yin, Y. Zhang, K. Sun, L. Xie et al., Two-dimensional $Ti_3C_2T_x$ /carbonized wood metacomposites with weakly negative permittivity. *Adv. Compos. Hybrid Mater.* **5**, 2369–2377 (2022). <https://doi.org/10.1007/s42114-022-00442-1>
155. Y. Chen, Y. Meng, J. Zhang, Y. Xie, H. Guo et al., Leakage proof, flame-retardant, and electromagnetic shield wood morphology genetic composite phase change materials for solar

- thermal energy harvesting. *Nano-Micro Lett.* **16**, 196 (2024). <https://doi.org/10.1007/s40820-024-01414-4>
156. Y. Pan, M. Dai, H. Zhao, N. Hu, Q. Guo et al., Wood-based composites with high electromagnetic interference shielding effectiveness and ultra-low reflection. *Coatings* **12**, 1117 (2022). <https://doi.org/10.3390/coatings12081117>
157. Y. Pan, S. Hu, X. Zheng, N. Hu, F. Qiu et al., Efficient electromagnetic interference shielding of three-dimensional hydrophobic Cu/wood/Cu porous composites. *J. Wood Chem. Technol.* **43**, 206–220 (2023). <https://doi.org/10.1080/02773813.2023.2213691>
158. Z. Shen, J. Feng, Preparation of thermally conductive polymer composites with good electromagnetic interference shielding efficiency based on natural wood-derived carbon scaffolds. *ACS Sustainable Chem. Eng.* **7**, 6259–6266 (2019). <https://doi.org/10.1021/acssuschemeng.8b06661>
159. T. Tang, Z. Wang, J. Guan, Guan Achievements and challenges of copper-based single-atom catalysts for the reduction of carbon dioxide to C^{2+} products. *Exploration*. **3**, 20230011 (2023). <https://doi.org/10.1002/EXP.20230011>
160. K. Ji, H. Zhao, J. Zhang, J. Chen, Z. Dai, Fabrication and electromagnetic interference shielding performance of open-cell foam of a Cu–Ni alloy integrated with CNTs. *Appl. Surf. Sci.* **311**, 351–356 (2014). <https://doi.org/10.1016/j.apsusc.2014.05.067>
161. Z. Leng, Z. Yang, X. Tang, M.H. Helal, Y. Qu et al., Progress in percolative composites with negative permittivity for applications in electromagnetic interference shielding and capacitors. *Adv. Compos. Hybrid Mater.* **6**, 195 (2023). <https://doi.org/10.1007/s42114-023-00778-2>
162. Y. Pan, Q. Guo, D. Yin, M. Dai, X. Yu et al., Micro-nano-architectonics of electroless Cu/Ni composite materials based on wood. *J. Inorg. Organomet. Polym. Mater.* **32**, 687–699 (2022). <https://doi.org/10.1007/s10904-021-02155-2>
163. J. Ruan, Z. Chang, H. Rong, T.S. Alomar, D. Zhu et al., High-conductivity nickel shells encapsulated wood-derived porous carbon for improved electromagnetic interference shielding. *Carbon* **213**, 118208 (2023). <https://doi.org/10.1016/j.carbon.2023.118208>
164. Y. Pan, M. Dai, Q. Guo, D. Yin, S. Hu et al., Construction of sandwich-structured Cu–Ni wood-based composites for electromagnetic interference shielding. *Chem. Eng. J.* **471**, 144301 (2023). <https://doi.org/10.1016/j.cej.2023.144301>
165. C. Liu, L. Xu, X. Xiang, Y. Zhang, L. Zhou et al., Achieving ultra-broad microwave absorption bandwidth around millimeter-wave atmospheric window through an intentional manipulation on multi-magnetic resonance behavior. *Nano-Micro Lett.* **16**, 176 (2024). <https://doi.org/10.1007/s40820-024-01395-4>
166. I. Karteri, M. Altun, M. Gunes, Electromagnetic interference shielding performance and electromagnetic properties of wood-plastic nanocomposite with graphene nanoplatelets. *J. Mater. Sci. Mater. Electron.* **28**, 6704–6711 (2017). <https://doi.org/10.1007/s10854-017-6364-1>
167. C. Chen, W. Feng, W. Wu, Y. Yu, G. Qian et al., A highly strong PEDOT modified wood towards efficient electromagnetic interference shielding. *Ind. Crops Prod.* **202**, 117109 (2023). <https://doi.org/10.1016/j.indcrop.2023.117109>
168. J. Chen, Z. Zhu, H. Zhang, S. Tian, S. Fu, Wood-derived nanostructured hybrid for efficient flame retarding and electromagnetic shielding. *Mater. Des.* **204**, 109695 (2021). <https://doi.org/10.1016/j.matdes.2021.109695>
169. S. Bhadra, D. Khastgir, N.K. Singha, J.H. Lee, Progress in preparation, processing and applications of polyaniline. *Prog. Polym. Sci.* **34**, 783–810 (2009). <https://doi.org/10.1016/j.progpolymsci.2009.04.003>
170. Z. Ma, R. Jiang, J. Jing, S. Kang, L. Ma et al., Lightweight dual-functional segregated nanocomposite foams for integrated infrared stealth and absorption-dominant electromagnetic interference shielding. *Nano-Micro Lett.* **16**, 223 (2024). <https://doi.org/10.1007/s40820-024-01450-0>
171. Y. Xu, X. Zhang, G. Wang, X. Zhang, J. Luo et al., Preparation of a strong soy protein adhesive with mildew proof, flame-retardant, and electromagnetic shielding properties via constructing nanophase-reinforced organic–inorganic hybrid structure. *Chem. Eng. J.* **447**, 137536 (2022). <https://doi.org/10.1016/j.cej.2022.137536>
172. X. Zhang, Z. Liu, L. Cai, X. Zhang, C. Long et al., Development of a strong and conductive soy protein adhesive by building a hybrid structure based on multifunctional wood composite materials. *J. Clean. Prod.* **412**, 137461 (2023). <https://doi.org/10.1016/j.jclepro.2023.137461>
173. H.-C. Zhang, C.-N. Yu, X.-Z. Li, L.-F. Wang, J. Huang et al., Recent developments of nanocellulose and its applications in polymeric composites. *ES Food Agrofor.* **9**, 1–14 (2022). <https://doi.org/10.30919/esfaf768>
174. Y. Yang, L. Zhang, J. Zhang, Y. Ren, H. Huo et al., Fabrication of environmentally, high-strength, fire-retardant biocomposites from small-diameter wood lignin *in situ* reinforced cellulose matrix. *Adv. Compos. Hybrid Mater.* **6**, 140 (2023). <https://doi.org/10.1007/s42114-023-00721-5>
175. X. Bi, M. Li, G. Zhou, C. Liu, R. Huang et al., High-performance flexible all-solid-state asymmetric supercapacitors based on binder-free MXene/cellulose nanofiber anode and carbon cloth/polyaniline cathode. *Nano Res.* **16**, 7696–7709 (2023). <https://doi.org/10.1007/s12274-023-5586-1>
176. O.M. Atta, S. Manan, M. Ul-Islam, A.A.Q. Ahmed, M.W. Ullah et al., Development and characterization of plant oil-incorporated carboxymethyl cellulose/bacterial cellulose/glycerol-based antimicrobial edible films for food packaging applications. *Adv. Compos. Hybrid Mater.* **5**, 973–990 (2022). <https://doi.org/10.1007/s42114-021-00408-9>
177. B.O.O. Boni, L. Lamboni, L. Mao, B.M. Bakadia, Z. Shi et al., *In vivo* performance of microstructured bacterial cellulose-silk sericin wound dressing: effects on fibrosis and scar formation. *Eng. Sci.* **19**, 175–185 (2022). <https://doi.org/10.30919/es8d700>
178. Z. Zhang, N. Abidi, L.A. Lucia, S. Yu, A “bird nest” bioinspired strategy deployed for inducing cellulose gelation without concomitant dissolution. *Adv. Compos. Hybrid Mater.* **6**, 178 (2023). <https://doi.org/10.1007/s42114-023-00745-x>



179. W. Liu, Q. Lin, S. Chen, H. Yang, K. Liu et al., Microencapsulated phase change material through cellulose nanofibrils stabilized Pickering emulsion templating. *Adv. Compos. Hybrid Mater.* **6**, 149 (2023). <https://doi.org/10.1007/s42114-023-00725-1>
180. X. Wang, Y. Zhang, J. Luo, T. Xu, C. Si et al., Printability of hybridized composite from maleic acid-treated bacterial cellulose with gelatin for bone tissue regeneration. *Adv. Compos. Hybrid Mater.* **6**, 134 (2023). <https://doi.org/10.1007/s42114-023-00711-7>
181. Z. Ding, Z. Tian, X. Ji, H. Dai, C. Si, Bio-inspired catalytic one-step prepared R-siloxane cellulose composite membranes with highly efficient oil separation. *Adv. Compos. Hybrid Mater.* **5**, 2138–2153 (2022). <https://doi.org/10.1007/s42114-022-00517-z>
182. F. Zhang, M. Lian, A. Alhadhrami, M. Huang, B. Li et al., Laccase immobilized on functionalized cellulose nanofiber/alginate composite hydrogel for efficient bisphenol A degradation from polluted water. *Adv. Compos. Hybrid Mater.* **5**, 1852–1864 (2022). <https://doi.org/10.1007/s42114-022-00476-5>
183. Y. Li, J. Guo, M. Li, Y. Tang, V. Murugadoss et al., Recent application of cellulose gel in flexible sensing—a review. *ES Food Agrofor.* **4**, 9–27 (2021). <https://doi.org/10.30919/esfaf466>
184. O.M. Atta, S. Manan, M. Ul-Islam, A.A.Q. Ahmed, M.W. Ullah et al., Silver decorated bacterial cellulose nanocomposites as antimicrobial food packaging materials. *ES Food Agrofor.* **6**, 12–26 (2021). <https://doi.org/10.30919/esfaf590>
185. Y. Duan, H. Yang, K. Liu, T. Xu, J. Chen et al., Cellulose nanofibril aerogels reinforcing polymethyl methacrylate with high optical transparency. *Adv. Compos. Hybrid Mater.* **6**, 123 (2023). <https://doi.org/10.1007/s42114-023-00700-w>
186. Z. Li, C. Wang, T. Liu, X. Ye, M. He et al., Interfacial interaction enhancement between biodegradable poly (butylene adipate-co-terephthalate) and microcrystalline cellulose based on covalent bond for improving puncture, tearing, and enzymatic degradation properties. *Adv. Compos. Hybrid Mater.* **6**, 69 (2023). <https://doi.org/10.1007/s42114-023-00638-z>
187. S. Khan, M. Ul-Islam, A. Fatima, S. Manan, W. Ahmad Khattak et al., Potential of food and agro-industrial wastes for cost-effective bacterial cellulose production: an updated review of literature. *ES Food Agrofor.* **13**, 905 (2023). <https://doi.org/10.30919/esfaf905>
188. H. Gu, X. Huo, J. Chen, S.M. El-Bahy, Z.M. El-Bahy et al., An overview of cellulose aerogel: classification and applications. *ES Food Agrofor.* **10**, 1–9 (2022). <https://doi.org/10.30919/esfaf782>
189. N. Al-Harbi, M. Ali Hussein, Y. Al-Hadeethi, A. Umar et al., Cellulose acetate-hydroxyapatite-bioglass-zirconia nanocomposite particles as potential biomaterial: synthesis, characterization, and biological properties for bone application. *Eng. Sci.* **17**, 70–82 (2021). <https://doi.org/10.30919/es8d528>
190. J. Xiong, Q. Hu, J. Wu, Z. Jia, S. Ge et al., Structurally stable electrospun nanofibrous cellulose acetate/chitosan biocomposite membranes for the removal of chromium ions from the polluted water. *Adv. Compos. Hybrid Mater.* **6**, 99 (2023). <https://doi.org/10.1007/s42114-023-00680-x>
191. J. Zhou, T. Yi, Z. Zhang, D.-G. Yu, P. Liu et al., Electrospun Janus core (ethyl cellulose// polyethylene oxide) @ shell (hydroxypropyl methyl cellulose acetate succinate) hybrids for an enhanced colon-targeted prolonged drug absorbance. *Adv. Compos. Hybrid Mater.* **6**, 189 (2023). <https://doi.org/10.1007/s42114-023-00766-6>
192. M. Ye, S. Wang, X. Ji, Z. Tian, L. Dai et al., Nanofibrillated cellulose-based superhydrophobic coating with antimicrobial performance. *Adv. Compos. Hybrid Mater.* **6**, 30 (2022). <https://doi.org/10.1007/s42114-022-00602-3>
193. R. Li, H. Lin, P. Lan, J. Gao, Y. Huang et al., Lightweight cellulose/carbon fiber composite foam for electromagnetic interference (EMI) shielding. *Polymers* **10**, 1319 (2018). <https://doi.org/10.3390/polym10121319>
194. T.W. Lee, S.E. Lee, Y.G. Jeong, Highly effective electromagnetic interference shielding materials based on silver nanowire/cellulose papers. *ACS Appl. Mater. Interfaces* **8**, 13123–13132 (2016). <https://doi.org/10.1021/acsami.6b02218>
195. G. Wang, D. Lai, X. Xu, Y. Wang, Lightweight, stiff and heat-resistant bamboo-derived carbon scaffolds with gradient aligned microchannels for highly efficient EMI shielding. *Chem. Eng. J.* **446**, 136911 (2022). <https://doi.org/10.1016/j.cej.2022.136911>
196. X. Zhu, J. Xu, F. Qin, Z. Yan, A. Guo et al., Highly efficient and stable transparent electromagnetic interference shielding films based on silver nanowires. *Nanoscale* **12**, 14589–14597 (2020). <https://doi.org/10.1039/d0nr03790g>
197. J. Liu, S. Lin, K. Huang, C. Jia, Q. Wang et al., A large-area AgNW-modified textile with high-performance electromagnetic interference shielding. *npj Flex. Electron.* **4**, 10 (2020). <https://doi.org/10.1038/s41528-020-0074-0>
198. M. Zhu, X. Yan, Y. Lei, J. Guo, Y. Xu et al., An ultrastrong and antibacterial silver nanowire/aligned cellulose scaffold composite film for electromagnetic interference shielding. *ACS Appl. Mater. Interfaces* **14**, 14520–14531 (2022). <https://doi.org/10.1021/acsami.1c23515>
199. Y. Xu, K. Qian, D. Deng, L. Luo, J. Ye et al., Electroless deposition of silver nanoparticles on cellulose nanofibrils for electromagnetic interference shielding films. *Carbohydr. Polym.* **250**, 116915 (2020). <https://doi.org/10.1016/j.carbpol.2020.116915>
200. Z. Cui, C. Gao, Z. Fan, J. Wang, Z. Cheng et al., Lightweight MXene/cellulose nanofiber composite film for electromagnetic interference shielding. *J. Electron. Mater.* **50**, 2101–2110 (2021). <https://doi.org/10.1007/s11664-020-08718-2>
201. Y.-J. Wan, P.-L. Zhu, S.-H. Yu, R. Sun, C.-P. Wong et al., Ultralight, super-elastic and volume-preserving cellulose fiber/graphene aerogel for high-performance electromagnetic interference shielding. *Carbon* **115**, 629–639 (2017). <https://doi.org/10.1016/j.carbon.2017.01.054>
202. B. Shan, Y. Wang, X. Ji, Y. Huang, Enhancing low-frequency microwave absorption through structural polarization

- modulation of MXenes. *Nano-Micro Lett.* **16**, 212 (2024). <https://doi.org/10.1007/s40820-024-01437-x>
203. G. Shao, D.A.H. Hanaor, X. Shen, A. Gurlo, Freeze casting: from low-dimensional building blocks to aligned porous structures—a review of novel materials, methods, and applications. *Adv. Mater.* **32**, e1907176 (2020). <https://doi.org/10.1002/adma.201907176>
204. S. Wang, X. Jin, Y. Yue, C. Mei, X. Xu et al., Biomimetic patternable polyhydroxyl nanocellulose/MXene films sequentially bridged through a synergistic hydrogen and ionic interaction with tunable multi-photoresponsive performances. *Chem. Eng. J.* **470**, 144225 (2023). <https://doi.org/10.1016/j.cej.2023.144225>
205. Z. Zhou, Q. Song, B. Huang, S. Feng, C. Lu, Facile fabrication of densely packed Ti_3C_2 MXene/nanocellulose composite films for enhancing electromagnetic interference shielding and electro-/ photothermal performance. *ACS Nano* **15**, 12405–12417 (2021). <https://doi.org/10.1021/acsnano.1c04526>
206. X. Zhang, K. Qian, J. Fang, S. Thaiboonrod, M. Miao et al., Synchronous deprotonation–protonation for mechanically robust chitin/aramid nanofibers conductive aerogel with excellent pressure sensing, thermal management, and electromagnetic interference shielding. *Nano Res.* **17**, 2038–2049 (2024). <https://doi.org/10.1007/s12274-023-6189-6>
207. Y. Han, M. He, J. Hu, P. Liu, Z. Liu et al., Hierarchical design of FeCo-based microchains for enhanced microwave absorption in C band. *Nano Res.* **16**, 1773–1778 (2023). <https://doi.org/10.1007/s12274-022-5111-y>
208. M. Culebras, G.A. Collins, A. Beaucamp, H. Geaney, M.N. Collins et al., Lignin/Si hybrid carbon nanofibers towards highly efficient sustainable Li-ion anode materials. *Eng. Sci.* **17**, 195–203 (2022). <https://doi.org/10.30919/es8d608>
209. Y. Xu, W. Li, T. Xu, G. Wang, W. Huan et al., Straightforward fabrication of lignin-derived carbon-bridged graphitic carbon nitride for improved visible photocatalysis of tetracycline hydrochloride assisted by peroxy monosulfate activation. *Adv. Compos. Hybrid Mater.* **6**, 197 (2023). <https://doi.org/10.1007/s42114-023-00779-1>
210. W. Hu, J. Zhang, B. Liu, C. Zhang, Q. Zhao et al., Synergism between lignin, functionalized carbon nanotubes and Fe_3O_4 nanoparticles for electromagnetic shielding effectiveness of tough lignin-based polyurethane. *Compos. Commun.* **24**, 100616 (2021). <https://doi.org/10.1016/j.coco.2020.100616>
211. S.-X. Wang, L. Yang, L.P. Stubbs, X. Li, C. He, Lignin-derived fused electrospun carbon fibrous mats as high performance anode materials for lithium ion batteries. *ACS Appl. Mater. Interfaces* **5**, 12275–12282 (2013). <https://doi.org/10.1021/am4043867>
212. D. Wang, Y. Wang, W. Wang, T. Li, J. Jiang et al., Modified alkaline lignin for ductile polylactide composites. *Compos. Commun.* **22**, 100501 (2020). <https://doi.org/10.1016/j.coco.2020.100501>
213. D. Wang, H. Yang, J. Yang, B. Wang, P. Wasnik et al., Efficient visible light-induced photodegradation of industrial lignin using silver–CuO catalysts derived from Cu-metal organic framework. *Adv. Compos. Hybrid Mater.* **6**, 138 (2023). <https://doi.org/10.1007/s42114-023-00708-2>
214. L. Mu, Y. Dong, L. Li, X. Gu, Y. Shi et al., Achieving high value utilization of bio-oil from lignin targeting for advanced lubrication. *ES Mater. Manuf.* **11**, 72–80 (2021). <https://doi.org/10.30919/esmm5f1146>
215. J. Xu, R. Liu, L. Wang, A. Pranovich, J. Hemming et al., Towards a deep understanding of the biomass fractionation in respect of lignin nanoparticle formation. *Adv. Compos. Hybrid Mater.* **6**, 214 (2023). <https://doi.org/10.1007/s42114-023-00797-z>
216. W. Pei, Y. Yusufu, Y. Zhan, X. Wang, J. Gan et al., Biosynthesizing lignin dehydrogenation polymer to fabricate hybrid hydrogel composite with hyaluronic acid for cartilage repair. *Adv. Compos. Hybrid Mater.* **6**, 180 (2023). <https://doi.org/10.1007/s42114-023-00758-6>
217. J. Zhang, Y. Qi, Y. Zhang, J. Duan, B. Liu et al., Lignin based flexible electromagnetic shielding PU synergized with graphite. *Fibres. Polym.* **22**, 1–8 (2021). <https://doi.org/10.1007/s12221-021-9227-6>
218. Z. Shi, G. Xu, J. Deng, M. Dong, V. Murugadoss et al., Structural characterization of lignin from *D.sinicus* by FTIR and NMR techniques. *Green Chem. Lett. Rev.* **12**, 235–243 (2019). <https://doi.org/10.1080/17518253.2019.1627428>
219. X. Liu, J. Zhou, Y. Xue, X. Lu, Structural engineering of hierarchical magnetic/carbon nanocomposites via *in situ* growth for high-efficient electromagnetic wave absorption. *Nano-Micro Lett.* **16**, 174 (2024). <https://doi.org/10.1007/s40820-024-01396-3>
220. C. Zhang, J. Zhang, B. Liu, B. Liu, Q. Wang et al., Lignin doped epoxy acrylate sandwich electromagnetic shielding material synergized with Fe_3O_4 and CNT. *J. Dispers. Sci. Technol.* **43**, 2209–2217 (2022). <https://doi.org/10.1080/01932691.2021.1929286>
221. B. Zhan, Y. Qu, X. Qi, J. Ding, J.-J. Shao et al., Mixed-dimensional assembly strategy to construct reduced graphene oxide/carbon foams heterostructures for microwave absorption, anti-corrosion and thermal insulation. *Nano-Micro Lett.* **16**, 221 (2024). <https://doi.org/10.1007/s40820-024-01447-9>
222. Z. Niu, F. Qu, F. Chen, X. Ma, B. Chen et al., Multifunctional integrated organic-inorganic-metal hybrid aerogel for excellent thermal insulation and electromagnetic shielding performance. *Nano-Micro Lett.* **16**, 200 (2024). <https://doi.org/10.1007/s40820-024-01409-1>
223. Y. Liu, X. Zhao, Z. Liu, B. Sun, X. Liu et al., Functionalized lignin nanoparticles assembled with MXene reinforced polypropylene with favorable UV-aging resistance, electromagnetic shielding effects and superior fire-safety. *Int. J. Biol. Macromol.* **265**, 130957 (2024). <https://doi.org/10.1016/j.ijbiomac.2024.130957>
224. Z. Han, Y. Niu, X. Shi, D. Pan, H. Liu et al., MXene@C-MWCNT adhesive silica nanofiber membranes enhancing electromagnetic interference shielding and thermal insulation performance in extreme environments. *Nano-Micro Lett.* **16**, 195 (2024). <https://doi.org/10.1007/s40820-024-01398-1>



225. B. Fei, H. Yang, J. Yang, D. Wang, H. Guo et al., Sustainable compression-molded bamboo fibers/poly(lactic acid) green composites with excellent UV shielding performance. *J. Mater. Sci. Technol.* **205**, 247–257 (2025). <https://doi.org/10.1016/j.jmst.2024.03.074>
226. S. Ge, G. Zheng, Y. Shi, Z. Zhang, A. Jazzar et al., Facile fabrication of high-strength biocomposite through Mg²⁺-enhanced bonding in bamboo fiber. *Giant* **18**, 100253 (2024). <https://doi.org/10.1016/j.giant.2024.100253>
227. B. Fei, D. Wang, N. AlMasoud, H. Yang, J. Yang et al., Bamboo fiber strengthened poly(lactic acid) composites with enhanced interfacial compatibility through a multi-layered coating of synergistic treatment strategy. *Int. J. Biol. Macromol.* **249**, 126018 (2023). <https://doi.org/10.1016/j.ijbiomac.2023.126018>
228. Q. Zhang, L. Ning, Y. Shen, M. Wang, C. Wang et al., Study on shielding effectiveness, electrical conductivity and thermal property of bamboo-plastic shielding composite based on Ni-Fe-P coated bamboo fibers. *Mater. Lett.* **268**, 127578 (2020). <https://doi.org/10.1016/j.matlet.2020.127578>
229. Q. Zhang, K. Wang, X. Chen, X. Tang, Q. Zhao et al., Biomass composite based on metallized bamboo fiber for electromagnetic interference shielding, joule heating, and solar heating. *Compos. Sci. Technol.* **243**, 110228 (2023). <https://doi.org/10.1016/j.compscitech.2023.110228>
230. Y. Zuo, W. Li, P. Li, W. Liu, X. Li et al., Preparation and characterization of polylactic acid-g-bamboo fiber based on *in situ* solid phase polymerization. *Ind. Crops Prod.* **123**, 646–653 (2018). <https://doi.org/10.1016/j.indcrop.2018.07.024>
231. K. Zhang, Z. Chen, L.M. Smith, G. Hong, W. Song et al., Polypyrrole-modified bamboo fiber/polylactic acid with enhanced mechanical, the antistatic properties and thermal stability. *Ind. Crops Prod.* **162**, 113227 (2021). <https://doi.org/10.1016/j.indcrop.2020.113227>
232. K. Zhang, Z. Chen, M. Boukhir, W. Song, S. Zhang, Bioinspired polydopamine deposition and silane grafting modification of bamboo fiber for improved interface compatibility of poly (lactic acid) composites. *Int. J. Biol. Macromol.* **201**, 121–132 (2022). <https://doi.org/10.1016/j.ijbiomac.2021.12.119>
233. Q. Zhang, L. Ning, C. Wang, M. Wang, Y. Shen et al., Fabrication and characterization of bio-based shielding material with dissimilar surface resistivity prepared by electroless Ni-Fe-P alloy plating on bamboo (*N. affinis*). *J. Mater. Sci. Mater. Electron.* **30**, 21064–21078 (2019). <https://doi.org/10.1007/s10854-019-02476-6>
234. Q. Zhang, K. Wang, X. Chen, X. Tang, Q. Zhao et al., Improving the thermal stability and functionality of bamboo fibers by electroless plating. *ACS Sustainable Chem. Eng.* **10**, 16935–16947 (2022). <https://doi.org/10.1021/acssuschemeng.2c06017>
235. J. Wang, X. Wu, Y. Wang, W. Zhao, Y. Zhao et al., Green, sustainable architectural bamboo with high light transmission and excellent electromagnetic shielding as a candidate for energy-saving buildings. *Nano-Micro Lett.* **15**, 11 (2022). <https://doi.org/10.1007/s40820-022-00982-7>
236. Q. Niu, X. Yue, Z. Guo, H. Yan, Z. Fang et al., Flame retardant bamboo fiber reinforced polylactic acid composites regulated by interfacial phosphorus-silicon aerogel. *Polymer* **252**, 124961 (2022). <https://doi.org/10.1016/j.polymer.2022.124961>
237. Y. Wu, K. Huang, X. Weng, R. Wang, P. Du et al., PVB coating efficiently improves the high stability of EMI shielding fabric with Cu/Ni. *Adv. Compos. Hybrid Mater.* **5**, 71–82 (2022). <https://doi.org/10.1007/s42114-021-00401-2>
238. Y. He, M. Zhou, M.H.H. Mahmoud, X. Lu, G. He et al., Multifunctional wearable strain/pressure sensor based on conductive carbon nanotubes/silk nonwoven fabric with high durability and low detection limit. *Adv. Compos. Hybrid Mater.* **5**, 1939–1950 (2022). <https://doi.org/10.1007/s42114-022-00525-z>
239. Z. Ma, Z. Zhang, F. Zhao, Y. Wang, A multifunctional coating for cotton fabrics integrating superior performance of flame-retardant and self-cleaning. *Adv. Compos. Hybrid Mater.* **5**, 2817–2833 (2022). <https://doi.org/10.1007/s42114-022-00464-9>
240. C. Stephen, B. Shivamurthy, M. Mohan, A.-H.I. Mourad, R. Selvam et al., Low velocity impact behavior of fabric reinforced polymer composites—A review. *Eng. Sci.* **18**, 75–97 (2022). <https://doi.org/10.30919/es8d670>
241. C. Hu, F. Wang, X. Cui, Y. Zhu, Recent progress in textile-based triboelectric force sensors for wearable electronics. *Adv. Compos. Hybrid Mater.* **6**, 70 (2023). <https://doi.org/10.1007/s42114-023-00650-3>
242. A.S. Desai, V. Dabir, A. Ashok, Z. Wu, H.M. Pathan et al., Microbicidal study of zinc oxide nanocomposites based coir geotextile with image processing. *ES Gen.* **3**, 1101 (2024). <https://doi.org/10.30919/esg1101>
243. L. Wang, X. Shi, J. Zhang, Y. Zhang, J. Gu, Lightweight and robust rGO/sugarcane derived hybrid carbon foams with outstanding EMI shielding performance. *J. Mater. Sci. Technol.* **52**, 119–126 (2020). <https://doi.org/10.1016/j.jmst.2020.03.029>
244. X. Peng, X. Meng, B. Yu, H. Chen, Z. Liu et al., Graphitized and flexible porous textile updated from waste cotton for wearable electromagnetic interference shielding. *Carbon* **207**, 144–153 (2023). <https://doi.org/10.1016/j.carbon.2023.02.044>
245. Y. Peng, J. Dong, J. Long, Y. Zhang, X. Tang et al., Thermally conductive and UV-EMI shielding electronic textiles for unrestricted and multifaceted health monitoring. *Nano-Micro Lett.* **16**, 199 (2024). <https://doi.org/10.1007/s40820-024-01429-x>
246. F. Huang, Z. Tian, H. Ma, Z. Ding, X. Ji et al., Combined alkali impregnation and poly dimethyl diallyl ammonium chloride-assisted cellulase absorption for high-efficiency pretreatment of wheat straw. *Adv. Compos. Hybrid Mater.* **6**, 230 (2023). <https://doi.org/10.1007/s42114-023-00789-z>
247. Y. Wang, X.-X. Ji, S. Liu, Z. Tian, C. Si et al., Effects of two different enzyme treatments on the microstructure of outer surface of wheat straw. *Adv. Compos. Hybrid Mater.* **5**, 934–947 (2022). <https://doi.org/10.1007/s42114-021-00395-x>

248. D. Skoda, J. Vilcakova, R.S. Yadav, B. Hanulikova, T. Capkova et al., Nickel nanoparticle-decorated reduced graphene oxide via one-step microwave-assisted synthesis and its lightweight and flexible composite with Polystyrene-block-poly(ethylene-ran-butylene)-block-polystyrene polymer for electromagnetic wave shielding application. *Adv. Compos. Hybrid Mater.* **6**, 113 (2023). <https://doi.org/10.1007/s42114-023-00692-7>
249. H. Cheng, L. Xing, Y. Zuo, Y. Pan, M. Huang et al., Constructing nickel chain/MXene networks in melamine foam towards phase change materials for thermal energy management and absorption-dominated electromagnetic interference shielding. *Adv. Compos. Hybrid Mater.* **5**, 755–765 (2022). <https://doi.org/10.1007/s42114-022-00487-2>
250. T. Li, M. Zhu, Z. Yang, J. Song, J. Dai et al., Wood composite as an energy efficient building material: guided sunlight transmittance and effective thermal insulation. *Adv. Energy Mater.* **6**, 1601122 (2016). <https://doi.org/10.1002/aenm.201601122>
251. J. Zhou, B. Wang, C. Xu, Y. Xu, H. Tan et al., Performance of composite materials by wood fiber/polydopamine/silver modified PLA and the antibacterial property. *J. Mater. Res. Technol.* **18**, 428–438 (2022). <https://doi.org/10.1016/j.jmrt.2022.02.113>
252. S. Sankaran, K. Deshmukh, M.B. Ahamed, S.K. Khadheer Pasha, Recent advances in electromagnetic interference shielding properties of metal and carbon filler reinforced flexible polymer composites: a review. *Compos. Part A Appl. Sci. Manuf.* **114**, 49–71 (2018). <https://doi.org/10.1016/j.compositesa.2018.08.006>
253. L.-X. Lu, X.-L. Wang, S.-L. Li, Y. Tang, X.-M. Mai, Thermal performance of *Lonicera rupicola* grass as a building insulation composite material. *Adv. Compos. Hybrid Mater.* **6**, 8 (2022). <https://doi.org/10.1007/s42114-022-00578-0>
254. B.S. Maddodi, A. Lathashri, S. Devesh, A.U. Rao, G.B. Shenoy et al., Repurposing plastic wastes in non-conventional engineered wood building bricks for constructional application—a mechanical characterization using experimental and statistical analysis. *Eng. Sci.* **18**, 329–336 (2022). <https://doi.org/10.30919/es8d696>
255. M. Weng, S. Liu, J. Su, W. Xu, J. Huang et al., Hydrophobic and antimicrobial polyimide based composite phase change materials with thermal energy storage capacity, applied as multifunctional construction material. *Eng. Sci.* **19**, 301–311 (2022). <https://doi.org/10.30919/es8e735>
256. S.N. Mahdi, T. Imjai, C. Wattapanich, R. Garcia, H. Kaur et al., Life cycle cost analysis of flexible pavements reinforced with geo-synthetics: a case study of new construction or repair overlays in Thailand's Roads. *Eng. Sci.* **28**, 1071 (2024). <https://doi.org/10.30919/es1071>
257. H.A. Colorado, E.I. Gutierrez-Velasquez, L.D. Gil, I.L. de Camargo, Exploring the advantages and applications of nanocomposites produced via vat photopolymerization in additive manufacturing: a review. *Adv. Compos. Hybrid Mater.* **7**, 1 (2023). <https://doi.org/10.1007/s42114-023-00808-z>
258. H.A. Colorado, J.M. Henkin, Fire-resistant plants: a review of plant morphology, tissues, habits, ecological adaptations, and other factors contributing to bioderived environmental solutions and technologies. *Eng. Sci.* **27**, 1024 (2023). <https://doi.org/10.30919/es1024>
259. M.V. Singh, A. Kumar, N. Bhatt, J. Ren, H. Hou et al., Impact of contaminated water on plants and animals: utilizing natural and chemical coagulants for treating contaminated water. *ES Energy Environ.* **23**, 1032 (2023). <https://doi.org/10.30919/esee1032>
260. J. Guo, S. Xi, Y. Zhang, X. Li, Z. Chen et al., Biomass-based electromagnetic wave absorption materials with unique structures: a critical review. *ES Food Agrofor.* **13**, 900 (2023). <https://doi.org/10.30919/esfaf900>
261. J. Cai, S. Xi, C. Zhang, X. Li, M.H. Helal et al., Overview of biomass valorization: Case study of nanocarbons, biofuels and their derivatives. *J. Agric. Food Res.* **14**, 100714 (2023). <https://doi.org/10.1016/j.jafr.2023.100714>
262. S.-S. Cho, S.-H. Song, I.-P. Hong, Analysis of the electromagnetic properties of eco-friendly transparent wood. *Microw. Opt. Techn. Lett.* **63**, 2237–2241 (2021). <https://doi.org/10.1002/mop.32385>
263. S. Fujiwara, K. Shima, K. Chiba, Fundamental characteristics and humidity control capacity of bamboo charcoal. *Mokuzai Gakkaishi* **49**, 333–341 (2003)
264. C. Chen, Z. Li, R. Mi, J. Dai, H. Xie et al., Rapid processing of whole bamboo with exposed, aligned nanofibrils toward a high-performance structural material. *ACS Nano* **14**, 5194–5202 (2020). <https://doi.org/10.1021/acsnano.9b08747>
265. Z. Li, C. Chen, R. Mi, W. Gan, J. Dai et al., A strong, tough, and scalable structural material from fast-growing bamboo. *Adv. Mater.* **32**, e1906308 (2020). <https://doi.org/10.1002/adma.201906308>

Publisher's Note Springer Nature remains neutral with regard to jurisdictional claims in published maps and institutional affiliations.

